# Long-term trends in aerosol properties derived from AERONET measurements

Zhenyu Zhang[1], Jing Li[1], Huizheng Che[2], Yueming Dong[1], Oleg Dubovik[3], Thomas Eck[4,5], Pawan Gupta[4], Brent Holben[4], Jhoon Kim[6], Elena Lind[4], Trailokya Saud[7], Sachchida Nand Tripathi[7], and Tong Ying[1]

[1]Laboratory for Climate and Ocean-Atmosphere Studies, Department of Atmospheric and Oceanic Sciences, School of Physics, Peking University, 100871, Beijing, China
[2]State Key Laboratory of Severe Weather & Key Laboratory of Atmospheric Chemistry, Chinese Academy of Meteorological Sciences, China Meteorological Administration, 100081, Beijing, China
[3]Laboratoire d'Optique Atmosphérique, CNRS/Université de Lille, Villeneuve- d'Ascq, 59650, France
[4]NASA Goddard Space Flight Center, Greenbelt, 20771 MD, USA
[5]Goddard Earth Sciences and Technology Center, University of Maryland Baltimore County, Baltimore, MD, USA
[6]Department of Atmospheric Science, Yonsei University, Seoul, 03722, Republic of Korea
[7]Indian Institute of Technology Kanpur, Kanpur, 208016, India

**Correspondence:** Jing Li (jing-li@pku.edu.cn)

**Abstract.**

Over the past two decades, remarkable changes in aerosol concentrations and compositions have been observed worldwide, especially over developing countries, potentially resulting in considerable changes in aerosol properties. The Aerosol Robotic Network (AERONET) offers high precision measurements of aerosol optical parameters over about 1700 stations globally, many of which have long-term measurements for one or more decades. Here we use AERONET Level 2.0 quality assured measurements to investigate long-term trends for aerosol optical depth (AOD) and Ångström exponent (AE) trends, and quality-controlled Level 1.5 inversion products to analyze trends of absorption aerosol optical depth (AAOD) and single scattering albedo (SSA) at stations with long-term records. We also classify the aerosol properties in these sites into 6 types, and analyze the trends of each type. Results reveal decreases in AOD over the majority of the stations, except for North India and the Arabian Peninsula, where AOD increased. AE (computed from the AOD within the range of 440-870 nm) decreased in Europe, eastern North America, and the Middle East, but increased over South Asia and western North America. The decreased AE over Europe and eastern North America is likely due to decreased fine-mode anthropogenic aerosols, whereas that over the Arabian Peninsula is attributed to increased dust activities. Conversely, increased AE over North India is probably attributed to increased anthropogenic emissions and decreased dust loading. Most stations in Europe, North America, East Asia, and South Asia exhibit negative trends in AAOD, whereas Solar_Village in the Arabian Peninsula has positive trends. SSA at most stations increases and exhibits opposite trends to AAOD, but with several stations in North America showing decreased SSA values. Trend analysis of different aerosol types further reveals the changes of different aerosol components that are related to AOD, AE, AAOD, and SSA trends. The reductions of aerosols in eastern North America mainly result from non-absorbing species. Reductions of both fine-mode absorbing species and non-absorbing aerosols are found over Europe and East Asia,

but the reduction of absorbing species is stronger than that of non-absorbing species. Increased aerosols in Kanpur over North India should be mainly comprised of fine-mode scattering species, whereas those in Solar_Village over the Arabian Peninsula are mainly dust. Weak seasonality is found in the trends of all aerosol parameters analyzed in this work.

## 1 Introduction

Aerosols are pivotal in the study of climate change due to their significant effects on the climate system. Understanding the climate effects of aerosols necessitates a comprehensive recognition of their optical and microphysical properties. Variations in aerosol loading and aerosol properties can result in disparate climate impacts, underscoring the importance of accurately comprehending these changes. For example, changes in aerosol loading can directly influence the intensity of aerosol forcing, while a rise in aerosol absorption could even shift the aerosol forcing from negative to positive (Hansen et al., 1997), remarkably altering their climate effects. To quantify the contribution of aerosols to climate variability effectively, it is thus crucial to understand and quantify the long-term change of aerosol properties.

Studies using satellite observations revealed continuous reductions in the loading of aerosols and their precursors in Europe, North America, South America, and Africa in the past several decades, but increases over South Asia and Middle East, as well as increases in 2000s and decreases in 2010s over East Asia (Krotkov et al., 2016; Mehta et al., 2016; Zhao et al., 2017; de Meij et al., 2012; Fioletov et al., 2023; Gupta et al., 2022). In situ measurements also suggested negative scattering and absorption coefficient trends in majority of the stations which are mainly located in Europe and North America, and revealed increased scattering aerosol fraction (represented by single scattering albedo, SSA) in Asia, eastern/northern Europe, and the Arctic, and negative SSA trends in central Europe and central North America (Collaud Coen et al., 2020). As satellite observations mainly provide aerosol loading products and may have drifts in long-term calibration which impact aerosol monitoring, and the spatial coverage of in situ measurements is quite limited, ground-based remote sensing networks provide a very accurate data source to analyze trends in multiple aerosol parameters worldwide. Xia (2011) examined 79 stations within the Aerosol Robotic Network (AERONET, Holben et al., 1998) with observations no less than six years, and found decreases in aerosol optical depth (AOD) and Ångström exponent (AE) in eastern North America and Europe. Ningombam et al. (2019) analyzed long-term AOD trends over 49 AERONET sites and 4 Sky radiometer Network (SKYNET, Takamura and Nakajima, 2004) sites, and reported decline in AOD over North-South America, Europe, the Arctic, and Australia.

However, these studies based on ground-based remote sensing data mainly focused on trends in AOD and AE, while analysis on other aerosol optical properties, such as SSA and absorption aerosol optical depth (AAOD), is still insufficient. Other studies focusing on trends of these parameters are mainly restricted to specific stations with long-term records, which is mainly because of the limited data availability of AERONET Level 2.0 data. Li et al. (2014) utilized quality-controlled AERONET Level 1.5 inversion measurements at 54 selected stations as well as Level 2.0 solar observations at 90 selected stations worldwide for the period 2000-2013 to analyze the trends of AOD, AE, SSA, and AAOD. Decreased AOD and AAOD trends, along with increased SSA trends, were consistently observed in Japan, Europe and North America. North America exhibited positive AE trends, whereas Europe showed negative AE trends. India was reported to experience increases in AOD, AE, and SSA. The

Arabian Peninsula was noted for experiencing increased AOD and AAOD, with decreases in AE and SSA. Eastern China was characterized by a positive SSA trend and a negative AAOD trend, without significant changes in AOD or AE.

A decade later, many regions have experienced significant changes in aerosol loading and compositions. For example, recent studies have highlighted considerable reductions in aerosol loadings in East Asia as evidenced by AERONET measurements (Yu et al., 2022; Ramachandran and Rupakheti, 2022; Eom et al., 2022) and satellite observations (Ramachandran et al., 2020; Krotkov et al., 2016; Mehta et al., 2016; Zhao et al., 2017; Fioletov et al., 2023; Li, 2020; Gupta et al., 2022). Substantial reductions in anthropogenic emissions have been observed in eastern North America (Krotkov et al., 2016), potentially contributing to a decrease in AE. Central Australia has seen reported increases in dust activities (Shao et al., 2013), aligning with observed increases in AOD and decreases in AE (Yang et al., 2021), which might also lead to positive AAOD and negative SSA trends. Some potential variations in aerosol optical properties in certain regions were not captured by Li et al. (2014), partly due to limitations in the spatial and temporal coverages of surface stations at that time, and recent changes in aerosol loadings and compositions might lead to different or reversed trends. AERONET has now expanded from 400 to over 1700 stations globally with longer records. The AERONET algorithm has also been updated to Version 3 with numerous improvements (Giles et al., 2019; Sinyuk et al., 2020). These progresses underscore the need to update trend analysis of AERONET data to capture recent shifts in aerosol optical properties and reflect advancements in data quality and network coverage.

In this study, we analyze AERONET Level 2.0 AOD and AE observations at 172 stations and Level 1.5 quality-controlled AAOD and SSA measurements at 72 stations. We also made a further attempt to categorize aerosol types and analyze the trends of each type. We hope that this study can provide a more recent reference to aerosol changes globally and facilitate the assessment of aerosol climate and environmental impacts.

## 2 Data and Methods

### 2.1 AERONET Data

The AERONET is a ground-based aerosol remote sensing network, providing long-term observations of aerosol optical and microphysical properties, covering most of the continental areas around the world (Holben et al., 1998). The AERONET AOD observations are derived from direct solar radiation at several wavelength bands mainly ranging from 340 nm to 1640 nm, while other aerosol properties, including SSA and AAOD, are derived from diffuse sky radiance at four wavelengths at 440, 675, 870, and 1020 nm (Dubovik and King, 2000). The AE parameter is calculated using AOD measurements within 440-870 nm interval (Eck et al., 1999; Giles et al., 2019). There is a series of quality assurance strategies for AERONET Level 2.0 data that ensure an AOD uncertainty of 0.01 (visible)-0.02 (UV) and an SSA uncertainty of 0.03 at $AOD_{440}$ (AOD at 440 nm) $\sim$ 0.4 (Holben et al., 2006; Giles et al., 2019; Sinyuk et al., 2020). However, as Level 2.0 quality assurance for inversion products requires a coincident AOD exceeding 0.4 at 440 nm, many stations do not have enough data samples to produce a long-term record. Therefore, considering both the data quality and data availability, we utilize the all-point Version 3 Level 2.0 direct measurements for AOD and AE, and quality-controlled Level 1.5 almucantar inversion products (see below for the quality control scheme) for other parameters. The description and uncertainties of these parameters are detailed in Sect. 2.2.

The stations are selected primarily based on the availability of an extensive data record for the purpose of estimating the long-term trends of aerosol properties. The Level 1.5 almucantar inversion products are first screened based on all the Level 2.0 quality assurance criteria except for the AOD threshold, such as solar zenith angle > $50°$, sky error < $5\%$, and coincident Level 2.0 AOD measurements. The Level 2.0 direct measurements and screened Level 1.5 almucantar inversion products are then used to calculate monthly measurements. We first remove outliers from all-point measurements, and then calculate the median of all-point measurements to represent the monthly value only if there are more than 5 all-point measurements in at least 3 different days for that month. To ensure adequate records in trend analysis, we require the data to have at least 10 years of records and no less than 8 monthly measurements for each year during the 2000-2022 period. For the years with at least 8 monthly measurements, the monthly medians are then averaged to annual and seasonal means, which are used to calculate annual and seasonal trends. Estimating a valid seasonal trend also requires at least a 10-year record. Considering polar stations often have no monthly measurements in winter, the least number of monthly medians for each year are reduced to 4 for stations at latitudes above 65 degrees. Specifically, the 2019-2022 data for Birdsville in Australia are eliminated for more accurate trend estimation, as these data are strongly biased due to a data filtering artifact in the quality assurance (QA) process of the algorithm according to Giles et al. (2019), which results in a large jump in AOD (personal communication, T. Eck). This AOD artifact is caused by erroneous time stamping of the data that is greatest at some sites in Australia due to a unique data logging system utilized there. The unnatural increase in AOD for Birdsville in 2019 can be found in Yang et al. (2021). As a result, 172 stations for the direct-sun observations and 72 stations for the inversion measurements are retained for trend analysis, covering all major continents over the world. Locations, trends and time series for all the stations could be found in the supplementary. The distributions of all the selected stations as well as the number of annual mean samples at each station are presented in Fig. 1. Locations of stations mentioned in this article are presented in Fig. 2.

Here we focus on analyzing AOD, SSA, and AAOD trends at 440 nm, which are noted as $AOD_{440}$, $SSA_{440}$, and $AAOD_{440}$, respectively. Trends for parameters at the other wavelengths are very similar and thus skipped. The AE is calculated from all AOD measurements within the 440-870 nm wavelength range (typically including 440, 500, 675, and 870 nm), and are commonly denoted as $AE_{440\_870}$.

### 2.2 Aerosol parameters

AOD represents the column aerosol extinction, directly reflecting the column loading and concentration of aerosols. AERONET Level 2.0 products provide very accurate AOD measurements at clear sky conditions, with an uncertainty of 0.01 at visible wavelengths. The patterns of AOD (Fig. 3) and AOD trends (Fig. 4) should be always kept in mind when analyzing trends of the other aerosol parameters, because uncertainties of the other parameters are closely related to AOD level (see below), whose trend reflect changes of aerosol loading.

The AE parameter describes the slope of the logarithm of AOD versus the logarithm of wavelength (Ångström, 1929), characterizing the wavelength dependency of AOD. AERONET $AE_{440\_870}$ products are calculated from the linear regression of AOD and wavelengths on a logarithmic scale within the range of 440-870 nm (Eck et al., 1999; Giles et al., 2019). The AE parameter closely correlates with aerosol particle size distribution, and is an indicator of aerosol components. For example,

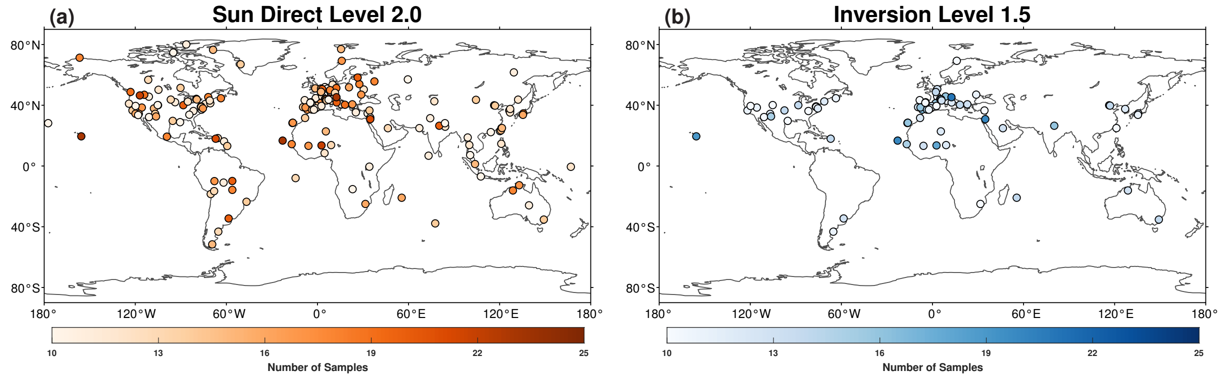


**Figure 1.** Locations of the stations selected for this study. (a) Level 2.0 solar stations, (b) Quality-controlled Level 1.5 almucantar stations. Color coding denotes the number of monthly samples for each station.

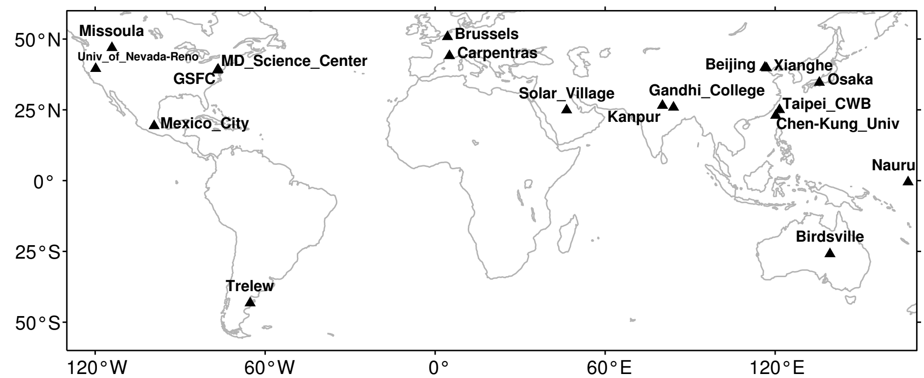


**Figure 2.** Locations of representative stations mentioned in the study.

dust particles typically have $AE_{440\_870}$ values around 0.3 or lower, and the $AE_{440\_870}$ for fine-mode particles that are mostly anthropogenic, usually exceed 1.0 (Farahat et al., 2016; Giles et al., 2012; Russell et al., 2010; Dubovik et al., 2002). Therefore, $AE_{440\_870}$ can reflect the relative fraction of fine and coarse mode particles. The error in AE can be estimated by the error in AOD as (Li et al., 2014; Kato et al., 2000):

$$\Delta\mathrm{AE} = \left[\frac{\sum_{i=1}^{n} e_i^2}{(n-2)\sum_{i=1}^{n}(\ln\lambda_i - \overline{\ln\lambda})^2}\right]^{\frac{1}{2}} \tag{1}$$

where $e_i$ is the error of the Ångström relationship, $n$ is the number of wavelengths $\lambda_i$ used to fit the Ångström relationship, and $\overline{\ln\lambda}$ is the average of the logarithm of the wavelengths. $e_i$ can be estimated using the relative error of AOD ($\frac{\Delta\mathrm{AOD}}{\mathrm{AOD}}$), and the uncertainty of AERONET AOD (ΔAOD) is considered as 0.01 here. According to Eq. 1, the uncertainty of AE is roughly inversely proportional to AOD, with larger errors at lower AOD conditions. Li et al. (2014) evaluated that the uncertainty of

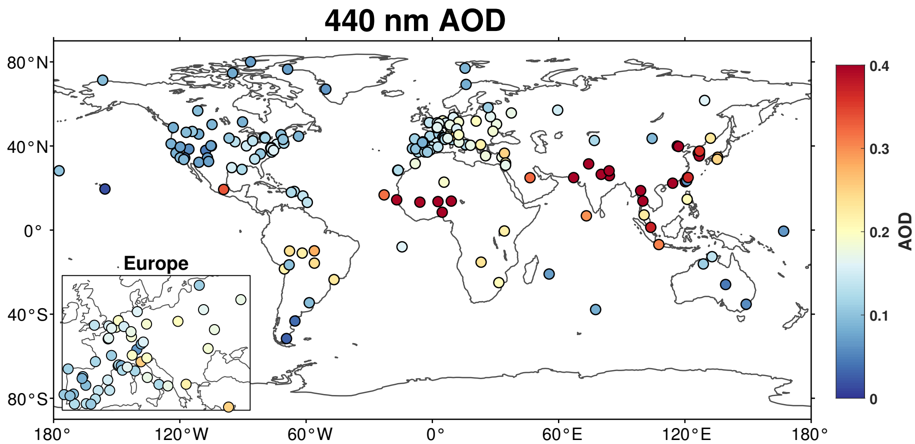


**Figure 3.** Mean AOD at 440 nm.

$AE_{440\_870}$ was $0.33$ when $AOD_{440} = 0.15$, and the uncertainty would rapidly increase to $0.56$ when $AOD_{440}$ decreased to $0.08$. Eck et al. (1999) also demonstrated significant variability in $AE_{440\_870}$ for lower AOD, largely attributed to increased relative errors in AOD at these low values. These results correspond to the inverse relationship between $\Delta AE$ and AOD. Therefore, it should be noted that $AE_{440\_870}$ is highly uncertain and the $AE_{440\_870}$ trends are less robust for sites with low AOD, even if the trends are statistically significant.

AAOD and SSA together characterize the scattering and absorbing properties of aerosols. AAOD represents the total aerosol absorption optical depth, whereas SSA reflects the relative contribution of scattering to total extinction. Therefore, the AAOD trend directly reflects changes in the amount of absorbing aerosols, while the SSA trend is related to variations of both absorbing and scattering aerosols. The relationship between the two parameters can be expressed as the following equation:

$$AAOD = (1 - SSA) \times AOD \tag{2}$$

The uncertainties of AAOD and SSA are also closely related to AOD level. AERONET implements a series of quality control criteria for Level 2.0 inversion products. Under these controls, AERONET SSA have an error of $\pm 0.03$ when $AOD_{440} \sim 0.4$, and the error increases rapidly (exponentially) at lower AOD levels, i.e., an error of $\pm 0.05$ when $AOD_{440} \sim 0.2$, and of $\pm 0.07$ when $AOD_{440} \sim 0.1$ (Sinyuk et al., 2020). Therefore, although we utilize all the Level 2.0 quality assurance criteria except for the AOD threshold for AAOD and SSA data, many of the SSA retrievals in this study have larger uncertainties of $\sim$ 0.03 to $\sim$ 0.09 due to low AOD level. Moreover, as SSA typically varies from approximately 0.8 to 1.0 (Dubovik et al., 2002; Giles et al., 2012), this error is remarkable when examining the variation of AAOD and SSA, i.e. a 0.03 error in SSA would lead to a 15% uncertainty. Therefore, the great uncertainties of AAOD and SSA should be kept in mind when analyzing their trends, especially for regions with low aerosol loadings.

## 2.3 Mann-Kendall test and Sen's slope for trend analysis

Here we use the Sen's slope combined with Mann-Kendall test to estimate the trend and its significance. The Mann-Kendall (MK) test (Mann, 1945; Kendall, 1975) is a nonparametric method to assess the significance of monotonic trends in a dataset without assuming any particular distribution. The slope of the trend $k$ can be estimated by the median of the set of slopes (Sen, 1968):

$$k = \text{Median}(\frac{Y_j - Y_i}{t_j - t_i}), \forall j > i \tag{3}$$

where $Y_i$ and $Y_j$ are the values of the variable at times $t_i$ and $t_j$, respectively.

The significance of the trend could be tested by calculating the MK statistic:

$$S = \sum_{i=1}^{n-1} \sum_{j=i+1}^{n} \text{sgn}(Y_j - Y_i) \tag{4}$$

where

$$\text{sgn}(x) = \begin{cases} -1 & \text{if } x < 0, \\ 0 & \text{if } x < 0, \\ 1 & \text{if } x > 0. \end{cases} \tag{5}$$

which has a normal distribution with zero mean and variance of (Li, 2020):

$$\sigma^2 = \frac{n(n-1)(2n+5) - \sum_{j=1}^{p} t_j(t_j - 1)(2t_j + 5)}{18} \tag{6}$$

The Sen's slope is a robust measurement of the trend in a dataset, and is not sensitive to outliers. As aerosol optical parameters do not follow a normal distribution, and AERONET records often have missing data, the Sen's slope is a good estimator of trends.

## 2.4 Aerosol Classification

In addition to the retrieved parameters, we also classify the observations into six aerosol types using the Fine Mode Fraction (FMF) at 550 nm and SSA at 440 nm (Lee et al., 2010). AOD and fine-mode AOD at 440, 675, 870, and 1020 nm are first interpolated to 550 nm using a second-order polynomial fit on a logarithmic scale (Eck et al., 1999). Then the $FMF_{550}$ is calculated by AOD and fine-mode AOD at 550 nm. The classification criteria for the six aerosol types ("Dust", "Mixture", and four fine-mode types), as well as the proportion of each type in the total number of quality-controlled Level 1.5 all-point record, are listed in Table 1. It should be noted that sea salt aerosols typically having $FMF_{550}$ below 0.4 and $SSA_{440}$ around 0.98 (included in the "Uncertain" type in Table 1) are not considered in the analysis of aerosol type trends (Sect. 3.3), because most AERONET stations are located over land where sea salt is not the predominant type, and sea salt aerosols only account for a negligible proportion (about 2.5% for "Uncertain" type).

**Table 1.** Criteria of aerosol classifications defined in Lee et al. (2010).

| Aerosol type | $FMF_{550}$ | $SSA_{440}$ | Proportion |
|---|---|---|---|
| Dust | $FMF_{550} < 0.4$ | $SSA_{440} \leq 0.95$ | 14.4% |
| Mixture | $0.4 \leq FMF_{550} \leq 0.6$ | / | 17.2% |
| Non-absorbing Fine (NA) | $FMF_{550} > 0.6$ | $SSA_{440} > 0.95$ | 22.6% |
| Slightly-absorbing Fine (SA) | $FMF_{550} > 0.6$ | $0.9 < SSA_{440} \leq 0.95$ | 21.6% |
| Moderately-absorbing Fine (MA) | $FMF_{550} > 0.6$ | $0.85 < SSA_{440} \leq 0.9$ | 11.4% |
| Highly-absorbing Fine (HA) | $FMF_{550} > 0.6$ | $SSA_{440} \leq 0.85$ | 10.3% |
| Uncertain | $FMF_{550} < 0.4$ | $SSA_{440} > 0.95$ | 2.5% |

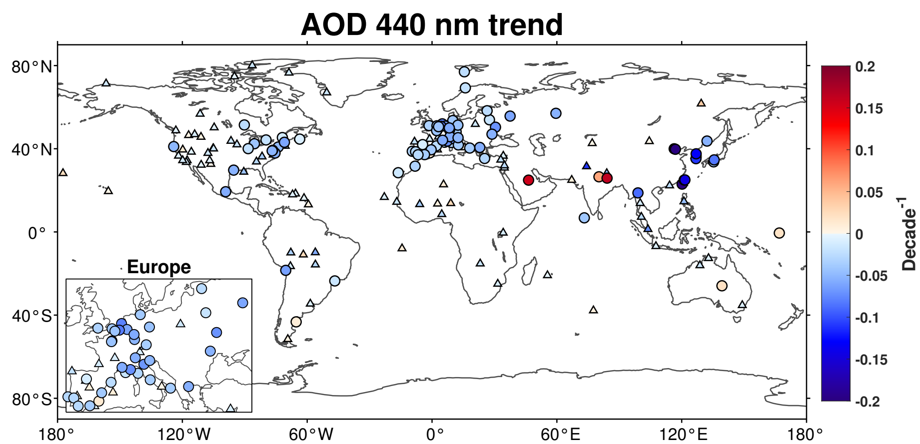


**Figure 4.** Trends of 440 nm AOD at AERONET stations. Triangles indicate trends below 90% significance level. Dots indicate trends at 90% significance. The magnitude of the trend has the unit of [per decade].

Each quality-controlled Level 1.5 inversion all-point measurement is classified as a specific aerosol type according to the classification criteria in Table 1. For each aerosol type, we use coincident Level 2.0 $AOD_{440}$ measurements to calculate the annual AOD and analyze its trend.

## 3 Results

### 3.1 Trends for AOD and AE

The $AOD_{440}$ trends at the 172 selected AERONET stations are presented in Fig. 4. Trends surpassing the 90% significance level are marked with dots. Trends below the 90% significance level are marked with triangles. The $AOD_{440}$ time series at several representative sites are shown in Fig. 5. Significant negative $AOD_{440}$ trends are found for the majority of stations all over the world, demonstrating a global reduction of aerosol loading. This result is consistent with previous studies (Li et al., 2014; Xia,

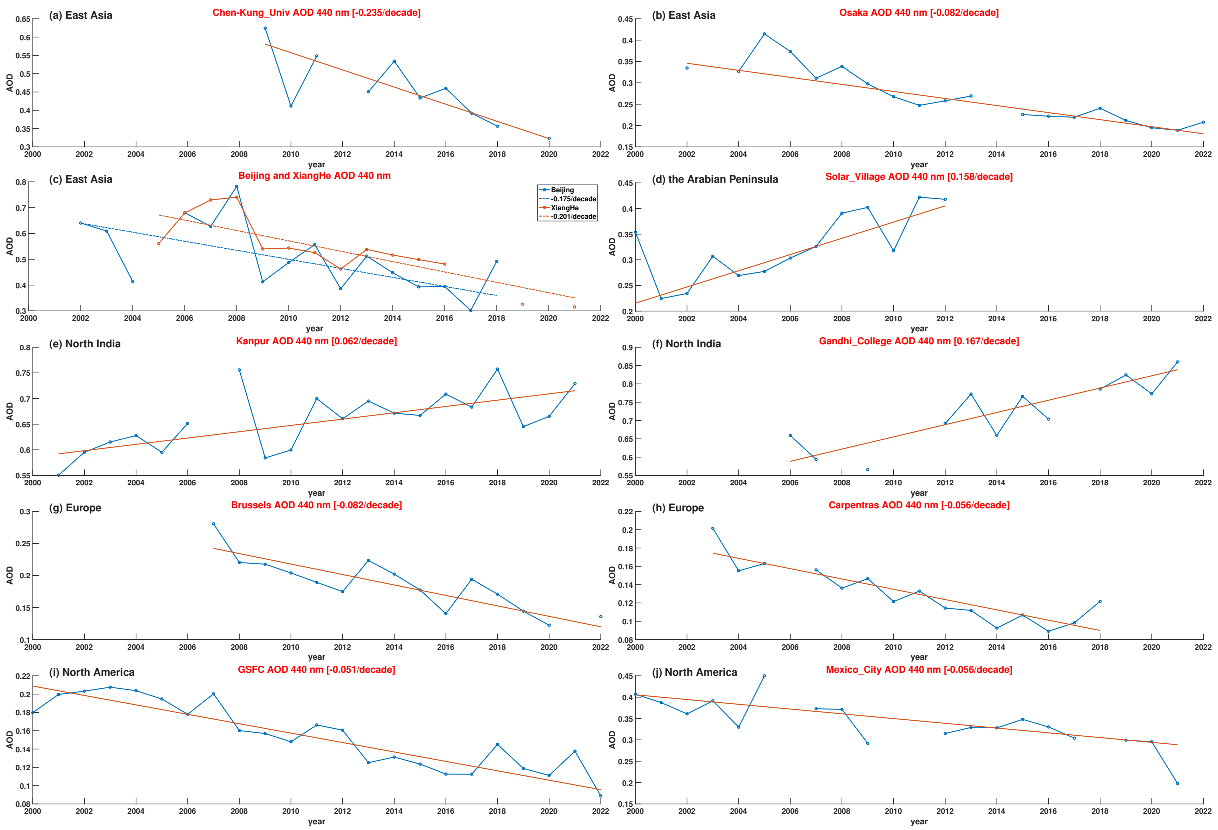


**Figure 5.** Time series of 440 nm AOD at several representative AERONET stations with trends at 90% significance. (a) Chen-Kung_Univ, (b) Osaka, (c) Beijing and XiangHe, (d) Solar_Village, (e) Kanpur, (f) Gandhi_College, (g) Brussels, (h) Carpentras, (i) GSFC, (j) Mexico_City.

2011; Ningombam et al., 2019). An increased number of stations with significant trends compared to these previous studies are observed in North America, Europe, and the Mediterranean, likely due to spatial and temporal expansion of the network in recent years. The rates of $AOD_{440}$ reduction in western Europe (about -0.05 per decade) are not as substantial as those reported in Li et al. (2014), which was -0.1 per decade, suggesting a decelerated aerosol reduction rate in Europe in recent years. This is also in line with the $AOD_{440}$ time series at representative European sites (Fig. 5g,h). Stations in the Arctic also exhibit coherent negative $AOD_{440}$ trends, consistent with previous studies (Breider et al., 2017; Wang et al., 2018). Since a significant proportion of aerosols in the Arctic are transported from lower latitudes, the reduction of aerosols in the Arctic is in line with the general reduction of AOD observed in the Northern Hemisphere. Strong negative $AOD_{440}$ trends are identified at more than 10 stations in East Asia and Southeast Asia, which were previously reported as exhibiting no significant trends in global studies (Li et al., 2014; Xia, 2011; Ningombam et al., 2019). The most considerable $AOD_{440}$ reductions are observed in East China, with significant declines exceeding -0.15 per decade at all the four stations (Chen-Kung_Univ, XiangHe, Taipei_CWB, and Beijing) and reaching -0.2 per decade at Chen-Kung_Univ and XiangHe. However, the trend of $AOD_{440}$ in East Asia is not coherent throughout the period of 2000-2022. According to the $AOD_{440}$ time series (Fig. 5a-c), $AOD_{440}$ increased in the early 2000s, and decreased rapidly in the later years since around 2008, consistent with other regional aerosol trend studies (Yoon et al., 2012; de Meij et al., 2012; Ramachandran and Rupakheti, 2022; Ramachandran et al., 2020; Eom et al., 2022; Li, 2020; Gupta et al., 2022; Lyapustin et al., 2011). This result also explains why Li et al. (2014) found no significant $AOD_{440}$ in East Asia with shorter records, as the increase of $AOD_{440}$ in the early 2000s offset the reduction after 2008. When applying longer records, the continuous reduction of $AOD_{440}$ after 2008 become dominant. A comparation between $AOD_{440}$ time series of XiangHe and Beijing (Fig. 5c), two stations located very close to each other in East China, would further reveal that the substantial reduction of $AOD_{440}$ mainly occurred in the later years. Both statons possess Level 2.0 records spanning a period of 17 years. However, the data record for Beijing, starting in 2002 and ending in 2018, reveals an $AOD_{440}$ trend of -0.175 per decade, whereas that for XiangHe, starting in 2005 and ending in 2021, is more recent and exhibits a larger $AOD_{440}$ decrease of -0.201 per decade, emphasizing the later years as a period of most notable $AOD_{440}$ reduction.

Significant positive $AOD_{440}$ trends are mainly found over Solar_Village in the Arabian Peninsula, and over Kanpur and Gandhi_College in North India. The Level 2.0 $AOD_{440}$ records at Solar_Village (Fig. 5d) ended in 2013, limiting current insights into aerosol properties in the Arabian Peninsula. Kanpur (Fig. 5e) has extensive records over the past two decades, exhibiting a positive $AOD_{440}$ trend of 0.062 per decade. This value is close to the trends calculated from different periods in previous studies (Ramachandran and Rupakheti, 2022; Li et al., 2014; Kaskaoutis et al., 2012; Kumar et al., 2022), indicating a steady increase in $AOD_{440}$ there. Compared to previous global studies, an additional station named Gandhi_College (Fig. 5f) in northern India is observed to have a significant positive $AOD_{440}$ trend of 0.167 per decade, indicating a more pronounced increase in aerosol loading in this region. Significant positive AERONET $AOD_{440}$ trends over the other regions, such as Birdsville in Australia, Trelew in South America, and Nauru, an oceanic island station, are generally weaker, with magnitudes typically below 0.03 per decade. As these sites have very low $AOD_{440}$ (typically below 0.1 for monthly values) as well as low $AOD_{440}$ variability, the results in these stations are typically more uncertain. The positive AOD trend for Birdsville in Australia was confirmed by the independent research conducted by Yang et al. (2021), however this was a false trend resulting from a previously mentioned data screening anomaly. In addition to Nauru which exhibits significant positive $AOD_{440}$ trend, some other oceanic stations worldwide also exhibit positive $AOD_{440}$ trends, suggesting a widespread increase in oceanic aerosols, primarily sea salts. This result is consistent with Hsu et al. (2012) who also reported an increase in oceanic AOD.

Significant negative $AE_{440\_870}$ trends are universally found for stations across Europe, the Mediterranean, eastern North America, and the Arabian Peninsula (Fig. 6, Fig. 7). In contrast, stations in western North America and North India mainly exhibit positive $AE_{440\_870}$ trends. The negative $AE_{440\_870}$ trends for Europe, the Mediterranean, and eastern North America are likely due to reductions in fine-mode anthropogenic aerosol and precursor emissions. In North India, considering the seasonal cycle of $AE_{440\_870}$ value, the positive $AE_{440\_870}$ trends for Kanpur and Gandhi_College primarily result from increased fine-mode anthropogenic emissions as well as decreased coarse-mode dust loading. These shifts in anthropogenic emissions have been assessed through satellite observations and emission inventories (Pouliot et al., 2015; Szymankiewicz et al., 2021; Krotkov et al., 2016; Zhao et al., 2017; de Meij et al., 2012; Kumar et al., 2021), and the decline of dust loading over South Asia was also verified by satellite observations and AERONET measurements (Pandey et al., 2016, 2017; Ramachandran and Rupakheti, 2022; Kaskaoutis et al., 2011). The Arabian Peninsula is a well-known dust source (Ginoux et al., 2012) and the $AE_{440\_870}$

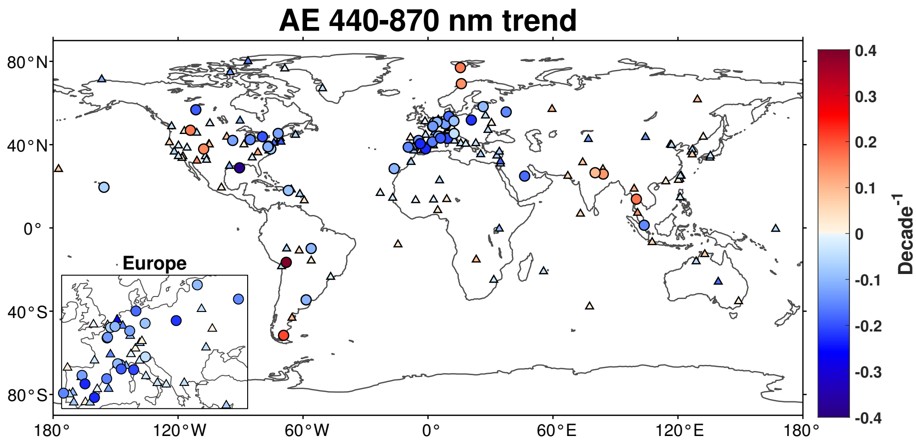


**Figure 6.** Same as Fig. 4, but with trends of AE.

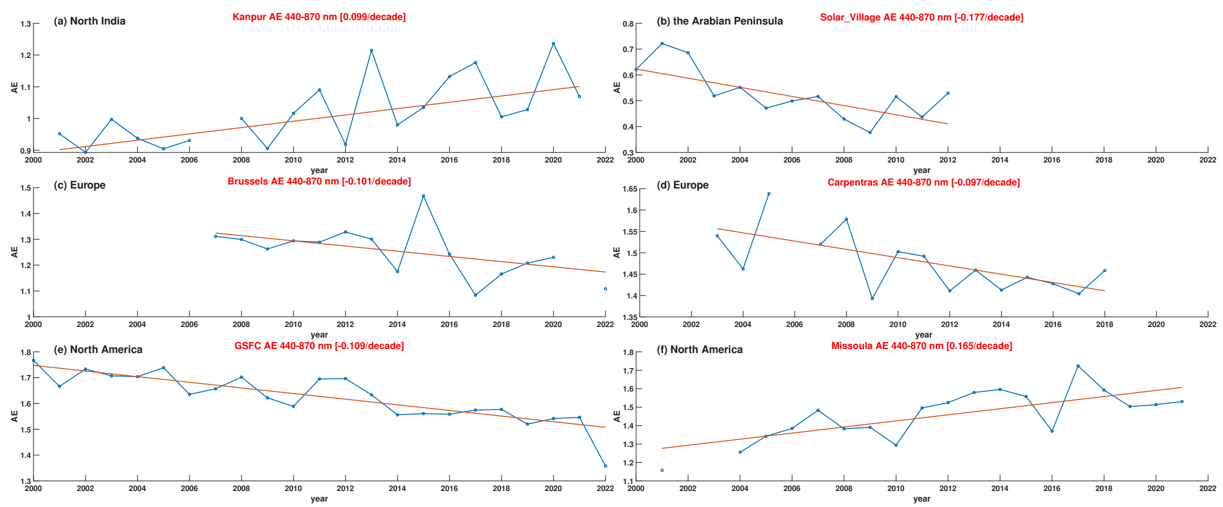


**Figure 7.** Time series of AE at several representative AERONET stations with trends at 90% significance. (a) Kanpur, (b) Solar_Village, (c) Brussels, (d) Carpentras, (e) GSFC, (f) Missoula.

values are typically low (Fig. 7b), therefore the negative $AE_{440\_870}$ trend for Solar_Village is likely attributed to increased dust activities. Conversely, the increased $AE_{440\_870}$ in western North America might be partly due to both increases in biomass burning aerosols and possibly diminished dust sources. These inferences align with previous studies, as Shao et al. (2013) also reported positive dust trends in the Middle East and negative trends in North America, whereas Eck et al. (2023) and Iglesias et al. (2022) revealed increases in biomass burning emissions over western North America. East Asia exhibits no significant $AE_{440\_870}$ trends, indicating weak changes in the ratio of fine-mode and coarse-mode aerosols. Therefore, the great decrease of aersol loading in East Asia revealed in Fig. 4 might be related to similar reductions in both anthropogenic fine-mode aerosols and coarse-mode dust in these areas.

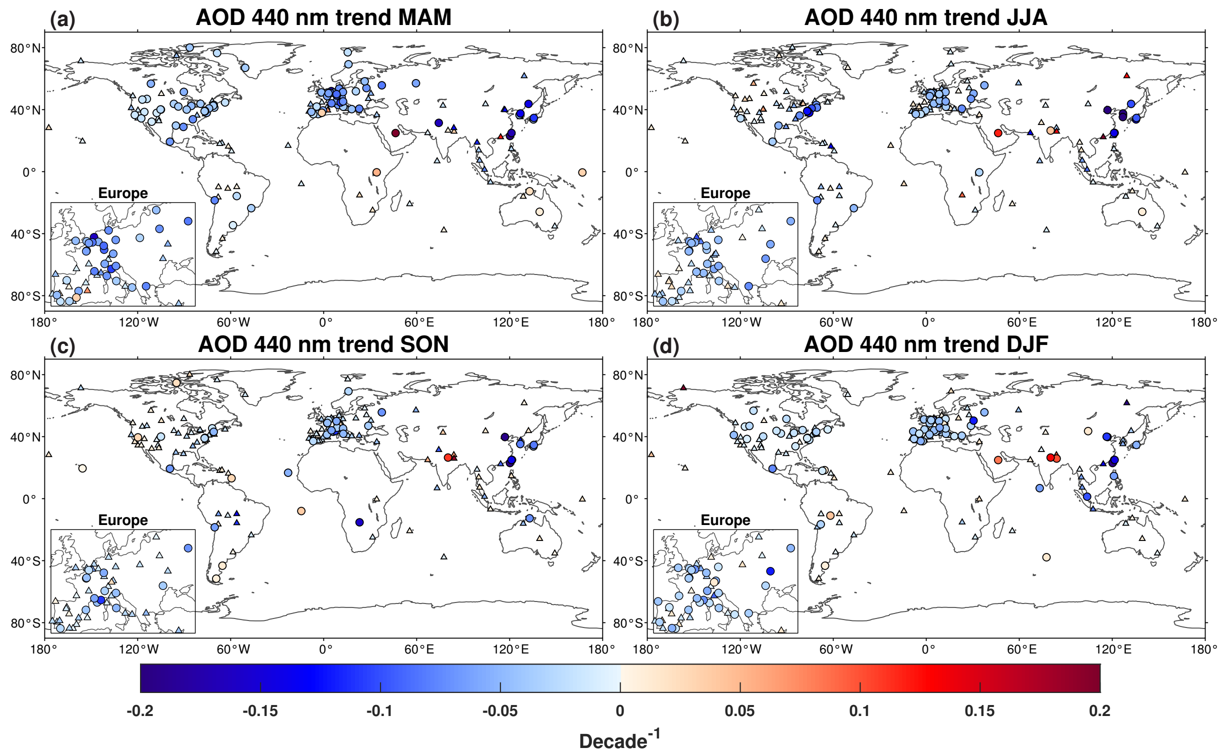


**Figure 8.** Seasonal trends of 440 nm AOD at AERONET stations. Triangles indicate trends below 90% significance level. Dots indicate trends at 90% significance. The magnitude of the trend has the unit of [per decade]. (a) pre-monsoon (South Asia, March-May), peak (the Arabian Peninsula, March-June), spring (other sites, March-May). (b) monsoon (South Asia, June-September), post-peak (the Arabian Peninsula, July-October), summer (West Africa, April-October), summer(other sites, June-August). (c) post-monsoon (South Asia, October-November), autumn(other sites, September-November). (d) winter (South Asia, December-February), pre-peak (the Arabian Peninsula, November-February), Harmattan (West Africa, November-March), winter(other sites, December-February)

The spatial distribution of seasonal $AOD_{440}$ (Fig. 8) and $AE_{440\_870}$ (Fig. 9) trends is generally similar to that of annual results. Nevertheless, the magnitude of the trends could vary by season, and certain stations might exhibit significant trends only during particular seasons. This variation is largely attributed to the seasonal patterns of aerosol emissions and meteorological conditions. For example, in Europe and North America, a greater number of stations exhibit significant $AOD_{440}$ trends in MAM (Fig. 8a), while $AE_{440\_870}$ trends in DJF (Fig. 9d) are more pronounced and deviate more from the annual results. Stations in the Arctic mainly exhibit significant negative $AOD_{440}$ trends in MAM. This is because aerosol concentrations are typically higher in spring and lower in winter in the Northern Hemisphere (see supplementary), allowing for more substantial reductions in spring and more significant compositional variations in winter. However, $AE_{440\_870}$ trends at low AOD seasons, such as the more pronounced $AE_{440\_870}$ trends in winter in the Northern Hemisphere, should be treated with caution, because the uncertainty in $AE_{440\_870}$ becomes large at low AOD conditions. In North India, Gandhi_College and Kanpur only exhibit significant $AOD_{440}$ trends during post-monsoon (October-November) (Fig. 8c) and winter (December-February) (Fig. 8d), while signifi-

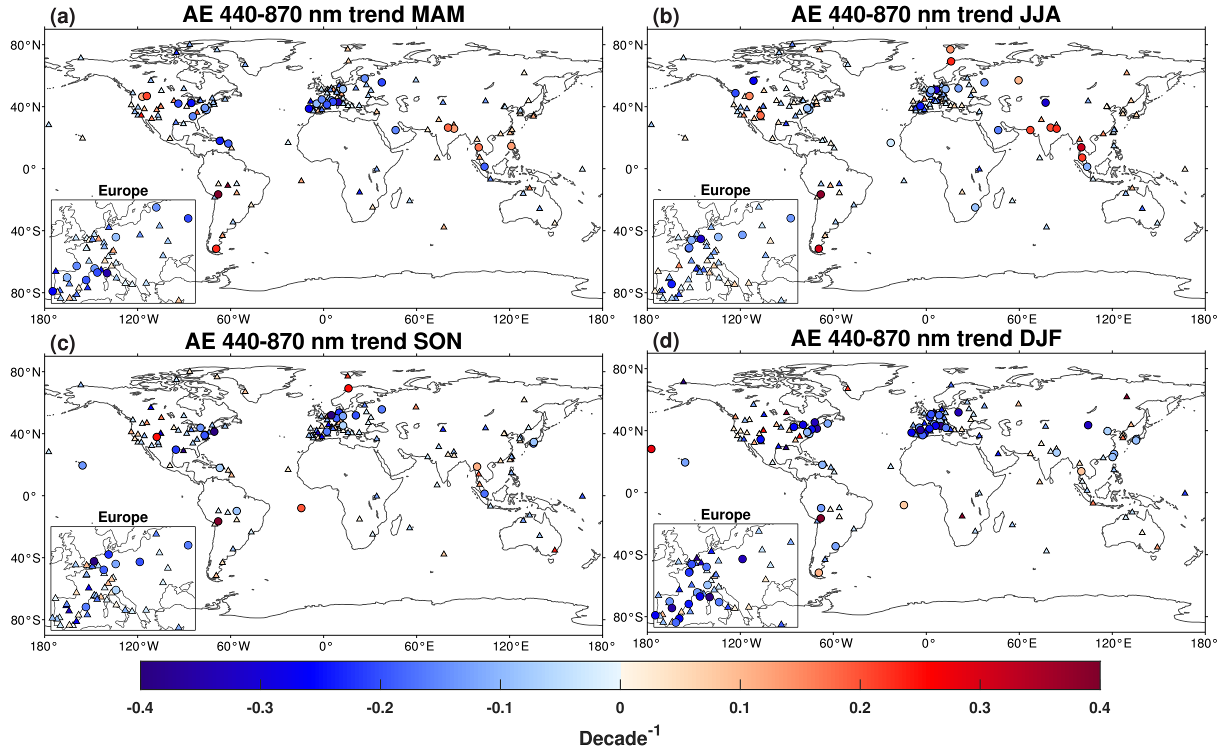


**Figure 9.** Same as Fig. 8, but with trends of AE.

cant $AE_{440\_870}$ trends predominantly occur in pre-monsoon (March-May) (Fig. 9a) and monsoon (June-September) (Fig. 9b). We can find that $AE_{440\_870}$ values at these stations in North India significantly exceed 1.0 in post-monsoon and winter, suggesting the predominance of fine-mode anthropogenic aerosols in these seasons. In contrast, $AE_{440\_870}$ values in pre-monsoon and monsoon start at approximately 0.5, emphasizing the dominance of coarse-mode aerosols, and rise to about 1.0 in recent years, suggesting a largely increased fraction of fine-mode aerosols. The seasonal patterns of AOD and AE in South Asia have also been verified through multi-year observations (Adhikary et al., 2007; Kaskaoutis et al., 2012). During the pre-monsoon and monsoon seasons, higher wind speeds and stronger precipitation lead to stronger dust activities and higher wet scavenging of aerosols, whereas in the post-monsoon and winter the meteorological conditions become reversed, with weaker dust activities and less efficient wet removal of aerosols occurred (Moorthy and Babu, 2006; Henriksson et al., 2011). As a result, in post-monsoon and winter, the rises in anthropogenic emissions, mainly crop residue burning in post-monsoon and biofuel and fossil fuel burning in winter (Yin, 2020; Bhardwaj et al., 2015; Venkataraman et al., 2018), have a negligible impact on changes in aerosol compositions and $AE_{440\_870}$ values, but would lead to the significant positive $AOD_{440}$ trends under less efficient wet removal. On the other hand, in pre-monsoon and monsoon, stronger wet scavenging of aerosols makes the AOD trend less pronounced, and the dominant aerosol type, dust, is mainly affected by natural variability (Kaskaoutis et al., 2012) and exhibits a negative trend (Pandey et al., 2017; Ramachandran and Rupakheti, 2022). Therefore, the increase in anthropogenic

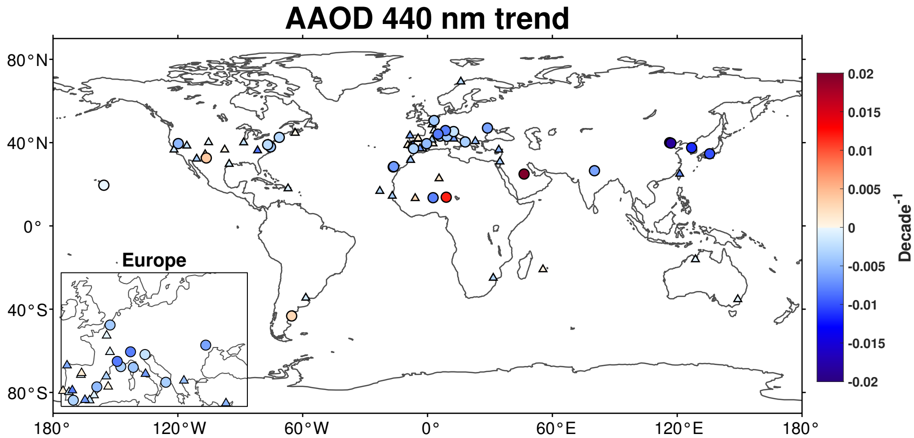


**Figure 10.** Same as Fig. 4, but with trends of AAOD.

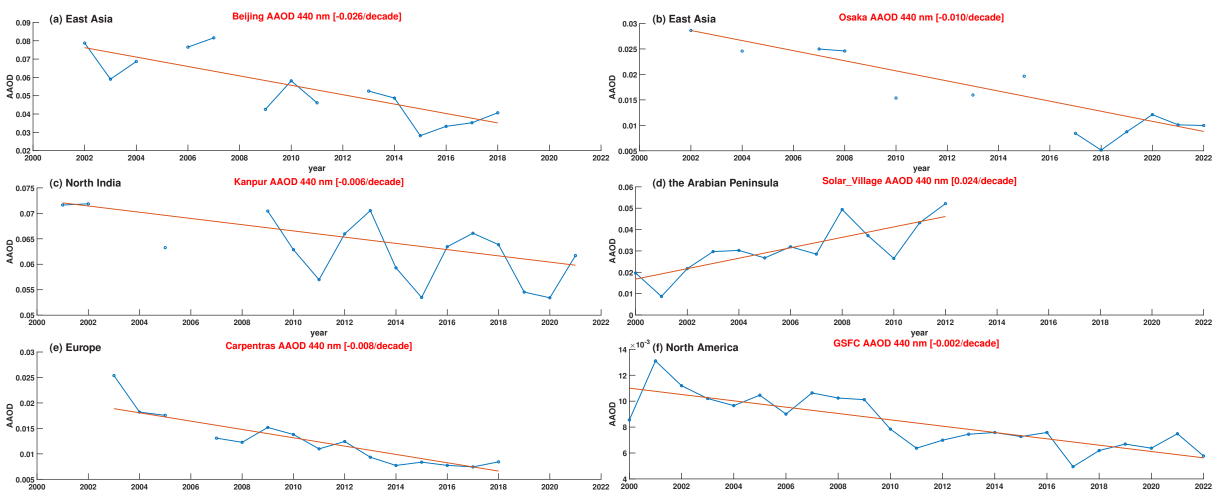


**Figure 11.** Time series of 440 nm AAOD at several representative AERONET stations with trends at 90% significance. (a) Beijing, (b) Osaka, (c) Kanpur, (d) Solar_Village, (e) Carpentras, (f) GSFC.

aerosols, i.e., biomass and biofuel burning emissions, fossil fuel emissions, and industry emissions (Venkataraman et al., 2018; Ramachandran and Rupakheti, 2022), does not have a significant impact on the total $AOD_{440}$ in these two seasons, but serves to increase the fine mode fractions, leading to the insignificant $AOD_{440}$ trends and significant positive $AE_{440\_870}$ trends.

## 3.2 Trends for AAOD and SSA

Similar to $AOD_{440}$, significant negative $AAOD_{440}$ trends (Fig. 10, Fig. 11) are universally found for AERONET stations in the Northern Hemisphere, especially in East Asia, North India, Europe and North America, indicating reductions in absorbing species, mainly primary aerosols. Conversely, significant positive $AAOD_{440}$ trend is mainly found for Solar_Village in the

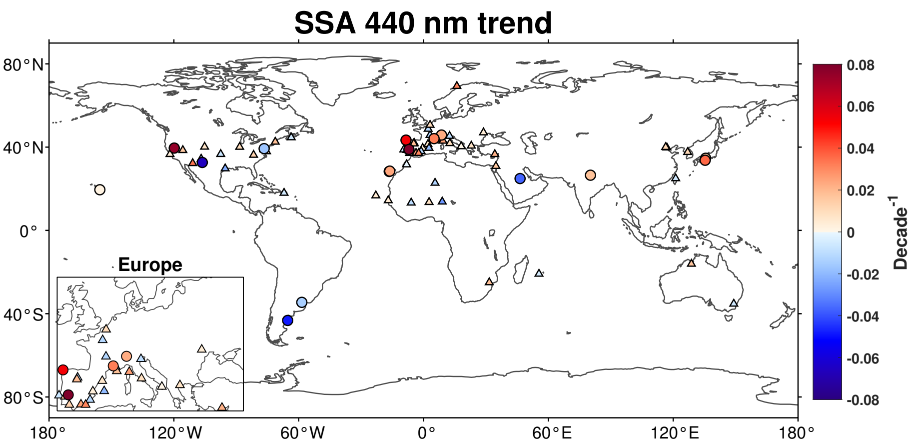


**Figure 12.** Same as Fig. 4, but with trends of SSA.

Arabian Peninsula (Fig. 11d), suggesting increases in absorbing aerosols. Trelew in southern South America also exhibits significant positive $AAOD_{440}$ trends, but the magnitude is very low and the results are relatively uncertain because the $AAOD_{440}$ are quite small. The reductions in $AAOD_{440}$ over East Asia, Europe, North India, and North America are primarily attributed to declines in anthropogenic emissions, such as reduced black carbon (BC) and/or organic carbon (OC) emissions from fossil fuels (Ramachandran and Rupakheti, 2022; He et al., 2023; Li et al., 2024), because aerosols in these regions are mainly of the Urban/Industrial type (Li et al., 2016). Decreased dust emissions discussed in the previous section might also be a potential contributor to the negative $AAOD_{440}$ trends in North India and westren North America (Shao et al., 2013; Zhang et al., 2019; Wang et al., 2021; Ramachandran and Rupakheti, 2022; Pandey et al., 2017), but the effect might not be as substantial as that of anthropogenic emissions, since dust is not the dominant type in these regions. Significant positive $AAOD_{440}$ trend for Solar_Village in the Arabian Peninsula is likely attributed to increased dust loading. As dust mainly exhibits strong absorption for short wavelengths, AAOD trends at other channels with longer wavelengths might not be that significant.

The $SSA_{440}$ trends (Fig. 12, Fig. 13) are generally opposite to the $AAOD_{440}$ trends, with exceptions in some stations in North America. Stations in North India, East Asia, and Europe, exhibit significant positive $SSA_{440}$ trends, corresponding to a decrease in the fraction of absorbing aerosols over time. The increase of $SSA_{440}$ in North India is attributed to both the decrease in absorbing species and a more pronounced increase in scattering aerosols. For East Asia and Europe, the positive $SSA_{440}$ trends suggest stronger reductions in absorbing species than scattering aerosols. $SSA_{440}$ trends show large spatial heterogeneity in North America. Significant positive $SSA_{440}$ trends are found for west coast, likely attributed to decreased absorbing aerosols. Significant negative trends are found over the center of the continent, corresponding to increase in absorbing aerosols. One station at east coast exhibits significant negative $SSA_{440}$ trend, which is likely attributed to great reduction in scattering aerosols such as sulfates, thereby increasing the proportion of absorbing aerosols. This result aligns with Collaud Coen et al. (2020), which also found SSA reductions in North America through in situ measurements, and attributed them to significant decreases in primarily scattering secondary aerosols. The substantial reductions in precursors of these scattering aerosols were also

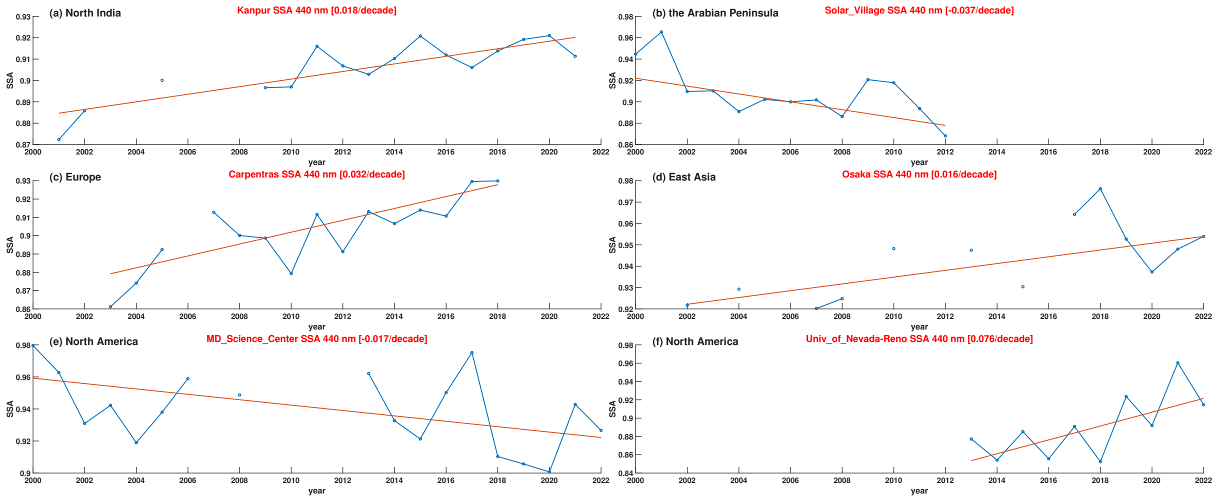


**Figure 13.** Time series of 440 nm SSA at several representative AERONET stations with trends at 90% significance. (a) Kanpur, (b) Solar_Village, (c) Carpentras, (d) Osaka, (e) MD_Science_Center, (f) Univ_of_Nevada-Reno.

confirmed by satellite observations and emission inventories (Szymankiewicz et al., 2021; Fioletov et al., 2023; Krotkov et al., 2016; Tong et al., 2015). However, several stations in eastern North America show positive trends which do not reaching the 90% significance threshold, emphasizing the spatial heterogeneity of $SSA_{440}$ trends in this area. Negative $SSA_{440}$ trend for Solar_Village (Fig. 13b) in the Arabian Peninsula is attributed to increases in absorbing dust aerosols.

Seasonally, although some stations exhibit significant trends primarily during particular seasons, the spatial patterns of seasonal $AAOD_{440}$ (Fig. 14) and $SSA_{440}$ (Fig. 15) trends are overall similar to those of annual trends. It is notable that Kanpur in North India exhibits stronger negative $AAOD_{440}$ trends during monsoon (Fig. 14b) where dust is the dominant aerosol type, further verifying that the decreased $AAOD_{440}$ is partly attributed to the decline in dust loading. As for $SSA_{440}$, the positive trends for Kanpur are significant at all the four seasons, indicating that the increased anthropogenic emissions in North India are mainly scattering species.

### 3.3 Aerosol type changes

To better explain the aerosol parameter changes, we make a further attempt to classify the measurements into six aerosol types as described in Sect. 2.4, and examine the long-term changes of the loadings for each type. The global $AOD_{440}$ trends of the six aerosol types are shown in Fig. 16.

Significant positive trend for "Dust" AOD is found for Solar_Village, suggesting increased dust activities over the Arabian Peninsula, which is consistent with analysis in previous sections and other studies using satellite observations and AERONET measurements (Mehta et al., 2016; Habib et al., 2019; Sabetghadam et al., 2021; Al Otaibi et al., 2019; Li et al., 2014). We do not find significant trends over other dust sources, as dust loading can have strong decadal variability which often does not yield monotonic trends. Dust trend can also be difficult to detect when combined with fine mode anthropogenic aerosols.

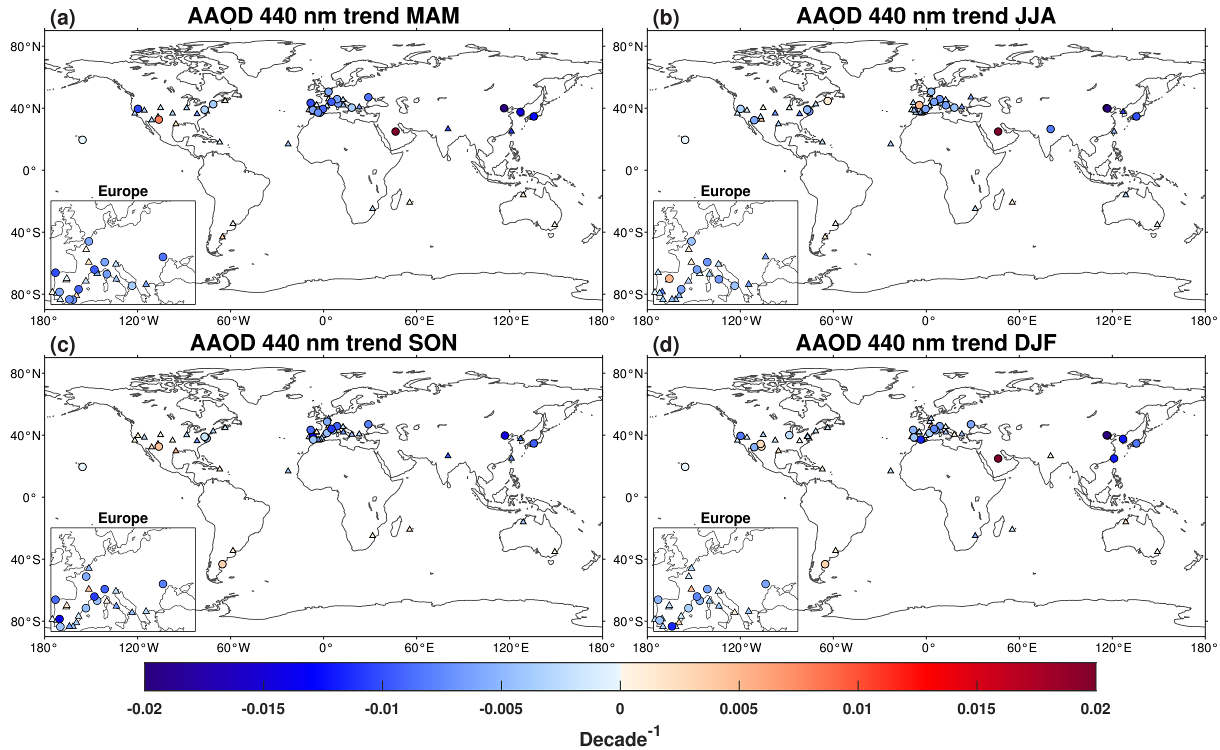


**Figure 14.** Same as Fig. 8, but with trends of AAOD.

The "Mixture" type straddles the boundary between "Dust" type and fine-mode types and is affected by both coarse-mode and fine-mode particles. Significant negative AOD trends in the "Mixture" type are mainly found over East Asia and Europe (Fig. 16b). Since East Asia and Europe are both predominated by fine-mode aerosols (Li et al., 2016; Zhang and Li, 2019), the decreased "Mixture" aerosols are thus primarily due to reductions in fine-mode anthropogenic emissions.

The majority of stations in Europe, North America, and East Asia exhibit significant negative AOD trends in four fine-mode types (Fig. 16c-f), corresponding to the reduction in both absorbing and scattering anthropogenic emissions revealed by the reductions in AOD (Fig. 4) and AAOD (Fig. 10) in these regions. The great reduction in absorbing types ("SA", "MA" and "HA") is also the possible reason for the increase of SSA (Fig. 12). It is notable that XiangHe in East Asia exhibits a significant positive trend in non-absorbing type ("NA") and even larger negative trends in the absorbing types, suggesting a great reduction in BC and/or OC emissions which might potentially lead to a shift in the predominance of aerosol type in pollution events (Zhang and Li, 2019). Eastern North America exhibits a greater reduction in non-absorbing aerosols than that in absorbing species, thus lead to an decrease in SSA (Fig. 12). Kanpur in North India exhibits significant positive trends on "SA" aerosols, and does not exhibit significant trends on other types. Compared to "MA" and "HA", the "SA" type is more scattering with lower BC proportion. As fine mode aerosols in Kanpur are initially absorbing types (Pandey et al., 2016), the increase in "SA" loading suggests a decreased proportion of BC, making the fine mode aerosols in this region more scattering.

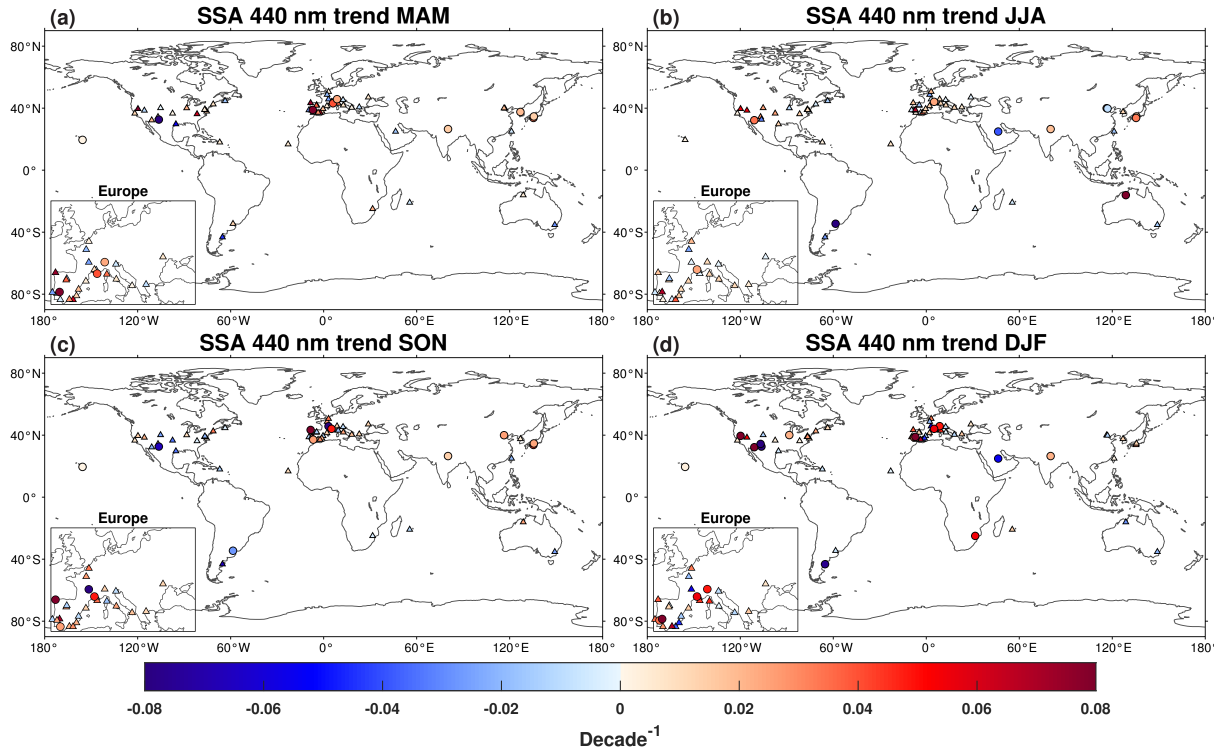


**Figure 15.** Same as Fig. 8, but with trends of SSA.

## 4 Discussion and Conclusion

In this study, we investigate trends in aerosol optical parameters using AERONET measurements. Globally, a universal decrease in AOD and AAOD, along with an increase in SSA, is observed at the majority of AERONET stations. The result generally aligns with the previous trend analysis using AERONET Version 2 products ending in 2013 (Li et al., 2014), highlighting the continuity of these trends over time on a global scale. Although our analysis is based on measurements at ground-based stations, coherent spatial patterns over different stations could also indicate regional features, which have also been demonstrated by satellite observations, model simulations, and emission inventories (Gupta et al., 2022; de Meij et al., 2012; Fioletov et al., 2023; Mishchenko et al., 2007; Wei et al., 2021b, a; Yoon et al., 2016). Although some regions, such as North India and western North America, have different seasonal and annual trends, the majority of regions do not exhibit significant seasonality. Taking advantages of longer records and improved station coverage, this study identifies more detailed regional trends and finds some new spatial patterns.

Spatially, significant negative $AOD_{440}$ trends are universally observed across East Asia and Southeast Asia. The most substantial reduction in $AOD_{440}$ occurs in East China, consistent with emission inventories (Kurokawa and Ohara, 2020). $AOD_{440}$ time series demonstrates that the pronounced decreases in aerosols within these regions are not coherent in the whole period, with aerosol loading increased in the early 2000s and decreased in the later years around 2008, which is also supported by

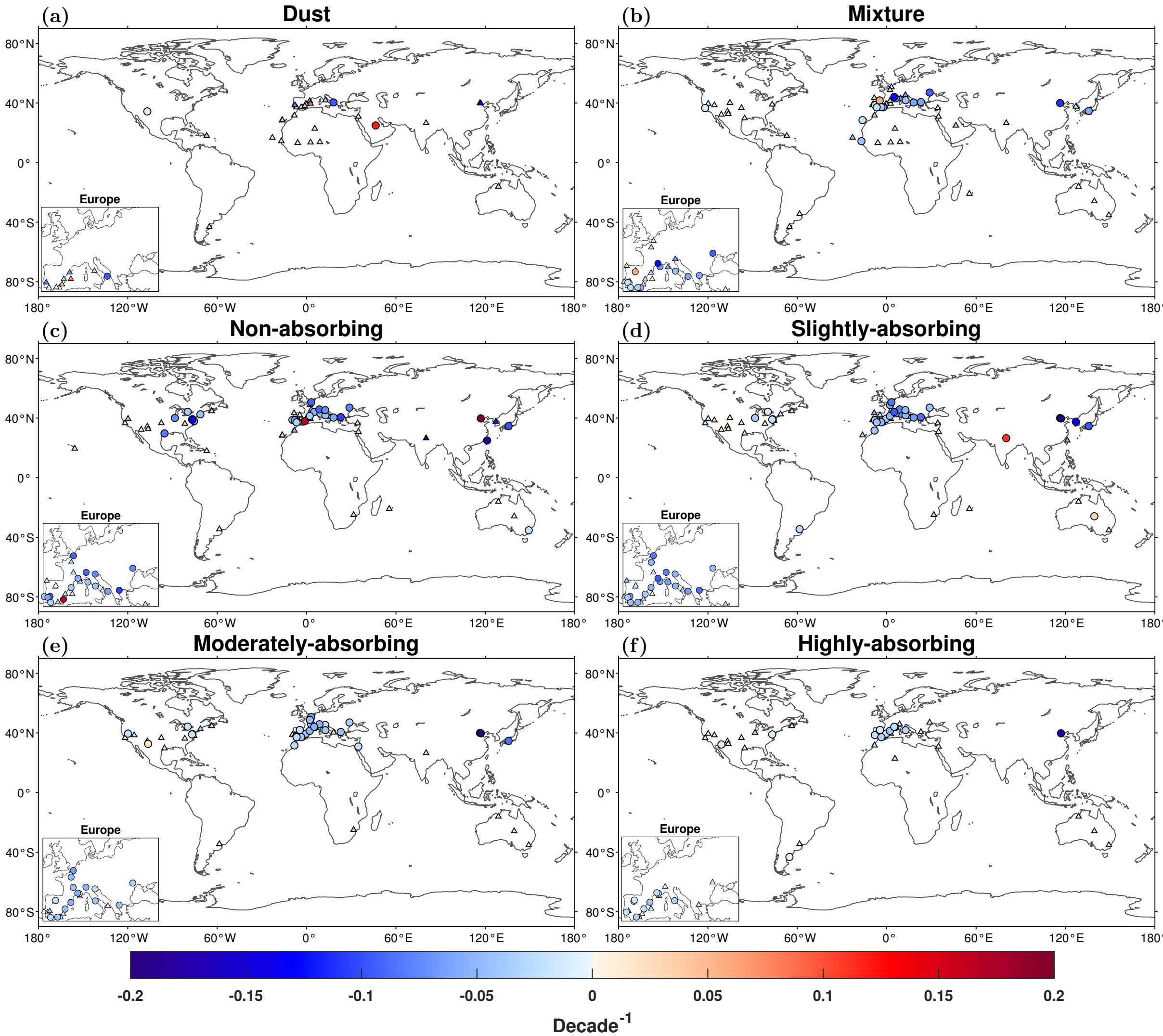


**Figure 16.** Same as Fig. 4, but with trends of AOD for 6 aerosol types. (a) dust, (b) Mixture, (c) Non-absorbing Fine, (d) Slightly-absorbing Fine, (e) Moderately-absorbing Fine, (f) Highly-absorbing Fine.

satellite observations and model simulations (Fioletov et al., 2023; de Meij et al., 2012; Zhao et al., 2017; Krotkov et al., 2016; Mehta et al., 2016). This study also finds significant negative $AAOD_{440}$ trends and positive $SSA_{440}$ trends for East Asia, which are mainly attributed to decreased absorbing primary aerosols, in agreement with other independent studies utilizing AERONET data (Ramachandran and Rupakheti, 2022; Ramachandran et al., 2020; Tao et al., 2017; Yu et al., 2022; Eom et al., 2022).

Coherent significant decreases of $AOD_{440}$ and $AAOD_{440}$ found for Europe and North America are in good agreement with satellite observations (Mehta et al., 2016; Zhao et al., 2017; Krotkov et al., 2016; Fioletov et al., 2023) as well as in situ measurements of recent aerosol absorbing and scattering trends (Collaud Coen et al., 2020). However, time series reveals diminished rates in the aerosol reduction in these regions. The decrease in anthropogenic emissions in Europe and North America started in the previous century and has led to a significant reduction in aerosol loading (de Meij et al., 2012; Szymankiewicz et al., 2021; Rafaj et al., 2013), resulting in a diminished rate of reduction in aerosol and aerosol precursor emissions over the last decade (Krotkov et al., 2016; Fioletov et al., 2023; Jiang et al., 2018). The observed decline in $AE_{440\_870}$ and increase in $SSA_{440}$ in Europe are also in line with previous studies and suggest reductions in anthropogenic emissions (Li et al., 2014; Xia, 2011). Significant negative $AE_{440\_870}$ trends are found for eastern North America, likely attributed to decline in anthropogenic emissions. Western North America exhibits significant positive $AE_{440\_870}$ trends which are likely related to reductions in dust emissions and increases in biomass burning emissions, consistent with dust monitoring results (Aryal and Evans, 2022) and trends in western North America forest fires (Eck et al., 2023; Iglesias et al., 2022). Significant negative $SSA_{440}$ trends are found for some stations over North America and align with those from in situ measurements conducted over similar periods (Collaud Coen et al., 2020), suggesting a larger decline in scattering aerosols than absorbing species.

Significant positive $AOD_{440}$ and $AE_{440\_870}$ trends are found for Kanpur and Gandhi_College in North India, highlighting an increase in fine-mode aerosols. We also find significant negative $AAOD_{440}$ trend and positive $SSA_{440}$ trend for Kanpur, indicating decreases in absorbing aerosols in this region, and we further attribute this change to both decreased anthropogenic BC emissions and decreased dust loading according to seasonal trend analysis and type analysis, consistent with previous studies (Pandey et al., 2016, 2017; Ramachandran and Rupakheti, 2022). These trends align with independent studies utilizing AERONET measurements (Ramachandran and Rupakheti, 2022; Kumar et al., 2022; Kaskaoutis et al., 2012) and satellite observations (Ramachandran et al., 2020; Kaskaoutis et al., 2011), together verifying the alteration of aerosol compositions and suggesting that the increased aerosols are mainly scattering fine-mode species. The trends over North India exhibit strong seasonality, with significant positive $AOD_{440}$ trends in post-monsoon and winter where anthropogenic aerosols are predominant, and decreased $AAOD_{440}$ and increased $AE_{440\_870}$ during pre-monsoon and monsoon where dust loading is stronger, suggesting that these seasonal trends may be associated with the seasonal cycle of aerosol emissions and meteorological conditions.

The AERONET products for Solar_Village end in 2013, therefore the trends of these aerosol optical parameters are the same as those reported by Li et al. (2014), with positive $AOD_{440}$ and $AAOD_{440}$ trends, and negative $AE_{440\_870}$ and $SSA_{440}$ trends, which is probably due to the increased dust activities in the Arabian Peninsula, and was also demonstrated in previous studies (Al Otaibi et al., 2019; Habib et al., 2019).

As a further step, we classify the aerosol observations into six types using $FMF_{550}$ and $SSA_{440}$, and examine the changes in aerosol loadings of each type. The trends for different aerosol types further verify the trends of AERONET parameters and offer insights into aerosol composition changes. We only find significant positive dust loading trend in the Arabian Peninsula. Significant trends mainly concentrate on fine-mode types, with declines in both absorbing types and the non-absorbing type globally, consistent with the negative $AOD_{440}$ and $AAOD_{440}$ trends. Spatially, the majority of stations in East Asia and Europe exhibit stronger reductions in absorbing aerosols than those in non-absorbing types, whereas in eastern North America the reduction in $AOD_{440}$ is mainly attributed to non-absorbing species. The results can fully explain the changes in $SSA_{440}$, which exhibit positive trends over East Asia and Europe and negative trends over eastern North America. Significant positive "SA" loading trend found in North India suggests a decrease in BC proportion which leads to increased $SSA_{440}$.

This study provides insights into temporal variations in aerosol loading, optical properties, and aerosol types. Decreases in AOD across Europe, North America, and East Asia reflect the effectiveness of emission control policies implemented in these regions. For instance, there has been a significant reduction in AOD over China in the past decade due to the Air Pollution Prevention and Control Action Plan (Gupta et al., 2022; Zhao et al., 2017). Conversely, the increase of AOD over North India and the Arabian Peninsula indicates deteriorating air quality, posing potential risks to public health. The substantial changes in SSA and AAOD observed in many regions are of concern for climate models due to their critical relationship with aerosol climate effects, potentially influencing regional energy budget, atmospheric circulation, the water cycle, etc. Previous studies have indicated that failure to capture the increase in SSA over northern India in climate models likely contributed to their biases in simulating the negative precipitation trend in this region (Ying et al., 2023). Furthermore, trends in aerosol properties and types are crucial for satellite remote sensing applications, as many algorithms rely on assumed aerosol models clustered from AERONET observations. Updating these models to reflect changes in aerosol types may be necessary (Zhang et al., 2024).

It is important to note that our analysis extends through 2022, encompassing the COVID-19 pandemic. Previous studies have documented significant reductions in aerosol loading and notable changes in aerosol compositions due to decreased anthropogenic emissions in regions implementing lockdown policies, such as East Asia, Europe, and North America (Cao et al., 2021; Clemente et al., 2022; Liang et al., 2023; Sokhi et al., 2021). We observed abnormally low AOD values at certain stations during this period, including XiangHe and Chen-Kung_Univ (Fig. 5a, c). This could potentially lead to a negative bias in AOD trends and contribute to discrepancies with other research on aerosol trends at these stations. However, since this period accounts for only about 10% of our total study period, and many stations lack Level 2.0 records for this time, the impact on trend analysis by COVID-19 is likely minimal at the majority of the stations.

The main purpose of this work is to update the trends in aerosol parameters with larger size of stations and longer records with respect to Li et al. (2014). We do note remarkable changes in aerosol trends over regions such as East Asia and the Southern Hemisphere, whereas patterns in other regions remain relatively stable. Most additional stations in this study are located in Europe and North America, where the distribution of stations is already dense to deduce general features of aerosol trends in these regions. We still lack insights into aerosol trends across other regions, including Asia, Africa, South America, Australia, and polar and oceanic regions where the spatial coverage of stations is insufficient, and some stations such as Solar_Village do not have Level 2.0 data in recent years. There is still need to establish more stations in Asia and the Southern Hemisphere to better capture the rapid change of aerosol properties there.

*Author contributions.* JL designed the research. TE, PG, BH, OD, and EL gathered the datasets and applied additional QAC to the data. ZZ selected the stations with long-term records, computed the trends, and analyzed the results. ZZ and JL prepared the manuscript draft. YD, TE, PG, SNT, and JK reviewed and edited the manuscript. All the other co-authors contributed to the measurements of aerosol optical properties applied in this work and to the manuscript review.

*Competing interests.* The authors declare that they have no conflict of interest.

*Acknowledgements.* We gratefully thank the AERONET team, especially the PIs and Co-Is and their staff of the 165 selected stations, for establishing and maintaining the sites and providing the data used in this study. The AERONET data are obtained from the AERONET website, https://aeronet.gsfc.nasa.gov/. This study is funded by the National Key Research and Development Program of China (grant no. 2023YFF0805401) and the National Natural Science Foundation of China (NSFC) Grants Nos. 42175144 and 42375121.

## References


Adhikary, B., Carmichael, G. R., Tang, Y., Leung, L. R., Qian, Y., Schauer, J. J., Stone, E. A., Ramanathan, V., and Ramana, M. V.: Characterization of the seasonal cycle of south Asian aerosols: A regional-scale modeling analysis, Journal of Geophysical Research: Atmospheres, 112, https://doi.org/10.1029/2006jd008143, 2007.

Al Otaibi, M., Farahat, A., Tawabini, B., Omar, M. H., Ramadan, E., Abuelgasim, A., and P. Singh, R.: Long-Term Aerosol Trends and Variability over Central Saudi Arabia Using Optical Characteristics from Solar Village AERONET Measurements, Atmosphere, 10, 752, https://doi.org/10.3390/atmos10120752, 2019.

Aryal, Y. and Evans, S.: Decreasing Trends in the Western US Dust Intensity With Rareness of Heavy Dust Events, Journal of Geophysical Research: Atmospheres, 127, https://doi.org/10.1029/2021jd036163, 2022.

Bhardwaj, P., Naja, M., Kumar, R., and Chandola, H. C.: Seasonal, interannual, and long-term variabilities in biomass burning activity over South Asia, Environmental Science and Pollution Research, 23, 4397–4410, https://doi.org/10.1007/s11356-015-5629-6, 2015.

Breider, T. J., Mickley, L. J., Jacob, D. J., Ge, C., Wang, J., Payer Sulprizio, M., Croft, B., Ridley, D. A., McConnell, J. R., Sharma, S., Husain, L., Dutkiewicz, V. A., Eleftheriadis, K., Skov, H., and Hopke, P. K.: Multidecadal trends in aerosol radiative forcing over the Arctic: Contribution of changes in anthropogenic aerosol to Arctic warming since 1980, Journal of Geophysical Research: Atmospheres, 122, 3573–3594, https://doi.org/10.1002/2016JD025321, 2017.

Cao, Y., Shao, L., Jones, T., Oliveira, M. L., Ge, S., Feng, X., Silva, L. F., and BéruBé, K.: Multiple relationships between aerosol and COVID-19: A framework for global studies, Gondwana Research, 93, 243–251, https://doi.org/10.1016/j.gr.2021.02.002, 2021.

Clemente, A., Yubero, E., Nicolás, J. F., Caballero, S., Crespo, J., and Galindo, N.: Changes in the concentration and composition of urban aerosols during the COVID-19 lockdown, Environmental Research, 203, 111 788, https://doi.org/10.1016/j.envres.2021.111788, 2022.

Collaud Coen, M., Andrews, E., Alastuey, A., Arsov, T. P., Backman, J., Brem, B. T., Bukowiecki, N., Couret, C., Eleftheriadis, K., Flentje, H., Fiebig, M., Gysel-Beer, M., Hand, J. L., Hoffer, A., Hooda, R., Hueglin, C., Joubert, W., Keywood, M., Kim, J. E., Kim, S.-W., Labuschagne, C., Lin, N.-H., Lin, Y., Lund Myhre, C., Luoma, K., Lyamani, H., Marinoni, A., Mayol-Bracero, O. L., Mihalopoulos, N., Pandolfi, M., Prats, N., Prenni, A. J., Putaud, J.-P., Ries, L., Reisen, F., Sellegri, K., Sharma, S., Sheridan, P., Sherman, J. P., Sun, J., Titos, G., Torres, E., Tuch, T., Weller, R., Wiedensohler, A., Zieger, P., and Laj, P.: Multidecadal trend analysis of in situ aerosol radiative properties around the world, Atmospheric Chemistry and Physics, 20, 8867–8908, https://doi.org/10.5194/acp-20-8867-2020, 2020.

de Meij, A., Pozzer, A., and Lelieveld, J.: Trend analysis in aerosol optical depths and pollutant emission estimates between 2000 and 2009, Atmospheric Environment, 51, 75–85, https://doi.org/10.1016/j.atmosenv.2012.01.059, 2012.

Dubovik, O. and King, M. D.: A flexible inversion algorithm for retrieval of aerosol optical properties from Sun and sky radiance measurements, Journal of Geophysical Research: Atmospheres, 105, 20 673–20 696, https://doi.org/10.1029/2000jd900282, 2000.

Dubovik, O., Holben, B., Eck, T. F., Smirnov, A., Kaufman, Y. J., King, M. D., Tanré, D., and Slutsker, I.: Variability of Absorption and Optical Properties of Key Aerosol Types Observed in Worldwide Locations, Journal of the Atmospheric Sciences, 59, 590–608, https://doi.org/10.1175/1520-0469(2002)059<0590:voaaop>2.0.co;2, 2002.

Eck, T. F., Holben, B. N., Reid, J. S., Dubovik, O., Smirnov, A., O'Neill, N. T., Slutsker, I., and Kinne, S.: Wavelength dependence of the optical depth of biomass burning, urban, and desert dust aerosols, Journal of Geophysical Research: Atmospheres, 104, 31 333–31 349, https://doi.org/10.1029/1999jd900923, 1999.

Eck, T. F., Holben, B. N., Reid, J. S., Sinyuk, A., Giles, D. M., Arola, A., Slutsker, I., Schafer, J. S., Sorokin, M. G., Smirnov, A., LaRosa, A. D., Kraft, J., Reid, E. A., O’Neill, N. T., Welton, E., and Menendez, A. R.: The extreme forest fires in California/Oregon in 2020: Aerosol optical and physical properties and comparisons of aged versus fresh smoke, Atmospheric Environment, 305, 119 798, https://doi.org/10.1016/j.atmosenv.2023.119798, 2023.

Eom, S., Kim, J., Lee, S., Holben, B. N., Eck, T. F., Park, S.-B., and Park, S. S.: Long-term variation of aerosol optical properties associated with aerosol types over East Asia using AERONET and satellite (VIIRS, OMI) data (2012–2019), Atmospheric Research, 280, 106 457, https://doi.org/10.1016/j.atmosres.2022.106457, 2022.

Farahat, A., El-Askary, H., Adetokunbo, P., and Fuad, A.-T.: Analysis of aerosol absorption properties and transport over North Africa and the Middle East using AERONET data, Annales Geophysicae, 34, 1031–1044, https://doi.org/10.5194/angeo-34-1031-2016, 2016.

Fioletov, V. E., McLinden, C. A., Griffin, D., Abboud, I., Krotkov, N., Leonard, P. J. T., Li, C., Joiner, J., Theys, N., and Carn, S.: Version 2 of the global catalogue of large anthropogenic and volcanic SO2 sources and emissions derived from satellite measurements, Earth System Science Data, 15, 75–93, https://doi.org/10.5194/essd-15-75-2023, 2023.

Giles, D. M., Holben, B. N., Eck, T. F., Sinyuk, A., Smirnov, A., Slutsker, I., Dickerson, R. R., Thompson, A. M., and Schafer, J. S.: An analysis of AERONET aerosol absorption properties and classifications representative of aerosol source regions, Journal of Geophysical Research: Atmospheres, 117, D17 203, https://doi.org/10.1029/2012jd018127, 2012.

Giles, D. M., Sinyuk, A., Sorokin, M. G., Schafer, J. S., Smirnov, A., Slutsker, I., Eck, T. F., Holben, B. N., Lewis, J. R., Campbell, J. R., Welton, E. J., Korkin, S. V., and Lyapustin, A. I.: Advancements in the Aerosol Robotic Network (AERONET) Version 3 database – automated near-real-time quality control algorithm with improved cloud screening for Sun photometer aerosol optical depth (AOD) measurements, Atmospheric Measurement Techniques, 12, 169–209, https://doi.org/10.5194/amt-12-169-2019, 2019.

Ginoux, P., Prospero, J. M., Gill, T. E., Hsu, N. C., and Zhao, M.: Global-scale attribution of anthropogenic and natural dust sources and their emission rates based on MODIS Deep Blue aerosol products, Reviews of Geophysics, 50, https://doi.org/10.1029/2012rg000388, 2012.

Gupta, G., Venkat Ratnam, M., Madhavan, B., and Narayanamurthy, C.: Long-term trends in Aerosol Optical Depth obtained across the globe using multi-satellite measurements, Atmospheric Environment, 273, 118 953, https://doi.org/10.1016/j.atmosenv.2022.118953, 2022.

Habib, A., Chen, B., Khalid, B., Tan, S., Che, H., Mahmood, T., Shi, G., and Butt, M. T.: Estimation and inter-comparison of dust aerosols based on MODIS, MISR and AERONET retrievals over Asian desert regions, Journal of Environmental Sciences, 76, 154–166, https://doi.org/10.1016/j.jes.2018.04.019, 2019.

Hansen, J., Sato, M., and Ruedy, R.: Radiative forcing and climate response, Journal of Geophysical Research: Atmospheres, 102, 6831–6864, https://doi.org/10.1029/96jd03436, 1997.

He, C., Niu, X., Ye, Z., Wu, Q., Liu, L., Zhao, Y., Ni, J., Li, B., and Jin, J.: Black carbon pollution in China from 2001 to 2019: Patterns, trends, and drivers, Environmental Pollution, 324, 121 381, https://doi.org/10.1016/j.envpol.2023.121381, 2023.

Henriksson, S. V., Laaksonen, A., Kerminen, V.-M., Räisänen, P., Järvinen, H., Sundström, A.-M., and de Leeuw, G.: Spatial distributions and seasonal cycles of aerosols in India and China seen in global climate-aerosol model, Atmospheric Chemistry and Physics, 11, 7975–7990, https://doi.org/10.5194/acp-11-7975-2011, 2011.

Holben, B. N., Eck, T. F., Slutsker, I., Tanré, D., Buis, J. P., Setzer, A., Vermote, E., Reagan, J. A., Kaufman, Y. J., Nakajima, T., Lavenu, F., Jankowiak, I., and Smirnov, A.: AERONET—A Federated Instrument Network and Data Archive for Aerosol Characterization, Remote Sensing of Environment, 66, 1–16, https://doi.org/10.1016/S0034-4257(98)00031-5, 1998.

Holben, B. N., Eck, T. F., Slutsker, I., Smirnov, A., Sinyuk, A., Schafer, J., Giles, D., and Dubovik, O.: Aeronet's Version 2.0 quality assurance criteria, in: Remote Sensing of the Atmosphere and Clouds, edited by Tsay, S.-C., Nakajima, T., Singh, R. P., and Sridharan, R., SPIE, ISSN 0277-786X, https://doi.org/10.1117/12.706524, 2006.

Hsu, N. C., Gautam, R., Sayer, A. M., Bettenhausen, C., Li, C., Jeong, M. J., Tsay, S.-C., and Holben, B. N.: Global and regional trends of aerosol optical depth over land and ocean using SeaWiFS measurements from 1997 to 2010, Atmospheric Chemistry and Physics, 12, 8037–8053, https://doi.org/10.5194/acp-12-8037-2012, 2012.

Iglesias, V., Balch, J. K., and Travis, W. R.: U.S. fires became larger, more frequent, and more widespread in the 2000s, Science Advances, 8, https://doi.org/10.1126/sciadv.abc0020, 2022.

Jiang, Z., McDonald, B. C., Worden, H., Worden, J. R., Miyazaki, K., Qu, Z., Henze, D. K., Jones, D. B. A., Arellano, A. F., Fischer, E. V., Zhu, L., and Boersma, K. F.: Unexpected slowdown of US pollutant emission reduction in the past decade, Proceedings of the National Academy of Sciences, 115, 5099–5104, https://doi.org/10.1073/pnas.1801191115, 2018.

Kaskaoutis, D. G., Kharol, S. K., Sinha, P. R., Singh, R. P., Badarinath, K. V. S., Mehdi, W., and Sharma, M.: Contrasting aerosol trends over South Asia during the last decade based on MODIS observations, https://doi.org/10.5194/amtd-4-5275-2011, 2011.

Kaskaoutis, D. G., Singh, R. P., Gautam, R., Sharma, M., Kosmopoulos, P. G., and Tripathi, S. N.: Variability and trends of aerosol properties over Kanpur, northern India using AERONET data (2001–10), Environmental Research Letters, 7, 024 003, https://doi.org/10.1088/1748-9326/7/2/024003, 2012.

Kato, S., Bergin, M. H., Ackerman, T. P., Charlock, T. P., Clothiaux, E. E., Ferrare, R. A., Halthore, R. N., Laulainen, N., Mace, G. G., Michalsky, J., and Turner, D. D.: A comparison of the aerosol thickness derived from ground-based and airborne measurements, Journal of Geophysical Research: Atmospheres, 105, 14 701–14 717, https://doi.org/10.1029/2000jd900013, 2000.

Kendall, M. G.: Rank correlation methods, Griffin, London [u.a.], 4. ed., 2. impr. edn., ISBN 0852641990, 1975.

Krotkov, N. A., McLinden, C. A., Li, C., Lamsal, L. N., Celarier, E. A., Marchenko, S. V., Swartz, W. H., Bucsela, E. J., Joiner, J., Duncan, B. N., Boersma, K. F., Veefkind, J. P., Levelt, P. F., Fioletov, V. E., Dickerson, R. R., He, H., Lu, Z., and Streets, D. G.: Aura OMI observations of regional $SO_2$ and $NO_2$ pollution changes from 2005 to 2015, Atmospheric Chemistry and Physics, 16, 4605–4629, https://doi.org/10.5194/acp-16-4605-2016, 2016.

Kumar, A., Pratap, V., Kumar, S., and Singh, A.: Atmospheric aerosols properties over Indo-Gangetic Plain: A trend analysis using ground – Truth AERONET data for the year 2009–2017, Advances in Space Research, 69, 2659–2670, https://doi.org/10.1016/j.asr.2021.12.052, 2022.

Kumar, S., Singh, A., Srivastava, A. K., Sahu, S. K., Hooda, R. K., Dumka, U. C., and Pathak, V.: Long-term change in aerosol characteristics over Indo-Gangetic Basin: How significant is the impact of emerging anthropogenic activities?, Urban Climate, 38, 100 880, https://doi.org/10.1016/j.uclim.2021.100880, 2021.

Kurokawa, J. and Ohara, T.: Long-term historical trends in air pollutant emissions in Asia: Regional Emission inventory in ASia (REAS) version 3, Atmospheric Chemistry and Physics, 20, 12 761–12 793, https://doi.org/10.5194/acp-20-12761-2020, 2020.

Lee, J., Kim, J., Song, C., Kim, S., Chun, Y., Sohn, B., and Holben, B.: Characteristics of aerosol types from AERONET sunphotometer measurements, Atmospheric Environment, 44, 3110–3117, https://doi.org/10.1016/j.atmosenv.2010.05.035, 2010.

Li, J.: Pollution Trends in China from 2000 to 2017: A Multi-Sensor View from Space, Remote Sensing, 12, 208, https://doi.org/10.3390/rs12020208, 2020.

Li, J., Carlson, B. E., Dubovik, O., and Lacis, A. A.: Recent trends in aerosol optical properties derived from AERONET measurements, Atmospheric Chemistry and Physics, 14, 12 271–12 289, https://doi.org/10.5194/acp-14-12271-2014, 2014.

Li, J., Li, X., Carlson, B. E., Kahn, R. A., Lacis, A. A., Dubovik, O., and Nakajima, T.: Reducing multisensor satellite monthly mean aerosol optical depth uncertainty: 1. Objective assessment of current AERONET locations, Journal of Geophysical Research: Atmospheres, 121, https://doi.org/10.1002/2016jd025469, 2016.

Li, W., Wang, Y., Yi, Z., Guo, B., Chen, W., Che, H., and Zhang, X.: Evaluation of MERRA-2 and CAMS reanalysis for black carbon aerosol in China, Environmental Pollution, 343, 123 182, https://doi.org/10.1016/j.envpol.2023.123182, 2024.

Liang, Y., Gui, K., Che, H., Li, L., Zheng, Y., Zhang, X., Zhang, X., Zhang, P., and Zhang, X.: Changes in aerosol loading before, during and after the COVID-19 pandemic outbreak in China: Effects of anthropogenic and natural aerosol, Science of The Total Environment, 857, 159 435, https://doi.org/10.1016/j.scitotenv.2022.159435, 2023.

Lyapustin, A., Smirnov, A., Holben, B., Chin, M., Streets, D. G., Lu, Z., Kahn, R., Slutsker, I., Laszlo, I., Kondragunta, S., Tanré, D., Dubovik, O., Goloub, P., Chen, H.-B., Sinyuk, A., Wang, Y., and Korkin, S.: Reduction of aerosol absorption in Beijing since 2007 from MODIS and AERONET, Geophysical Research Letters, 38, L10 803, https://doi.org/10.1029/2011gl047306, 2011.

Mann, H. B.: Nonparametric Tests Against Trend, Econometrica, 13, 245, https://doi.org/10.2307/1907187, 1945.

Mehta, M., Singh, R., Singh, A., Singh, N., and Anshumali: Recent global aerosol optical depth variations and trends — A comparative study using MODIS and MISR level 3 datasets, Remote Sensing of Environment, 181, 137–150, https://doi.org/10.1016/j.rse.2016.04.004, 2016.

Mishchenko, M. I., Geogdzhayev, I. V., Rossow, W. B., Cairns, B., Carlson, B. E., Lacis, A. A., Liu, L., and Travis, L. D.: Long-Term Satellite Record Reveals Likely Recent Aerosol Trend, Science, 315, 1543–1543, https://doi.org/10.1126/science.1136709, 2007.

Moorthy, K. K. and Babu, S. S.: Aerosol black carbon over Bay of Bengal observed from an island location, Port Blair: Temporal features and long-range transport, Journal of Geophysical Research: Atmospheres, 111, https://doi.org/10.1029/2005jd006855, 2006.

Ningombam, S. S., Larson, E., Dumka, U., Estellés, V., Campanelli, M., and Steve, C.: Long-term (1995–2018) aerosol optical depth derived using ground based AERONET and SKYNET measurements from aerosol aged-background sites, Atmospheric Pollution Research, 10, 608–620, https://doi.org/10.1016/j.apr.2018.10.008, 2019.

Pandey, S. K., Bakshi, H., and Vinoj, V.: Recent changes in dust and its impact on aerosol trends over the Indo-Gangetic Plain (IGP), in: Remote Sensing of the Atmosphere, Clouds, and Precipitation VI, edited by Im, E., Kumar, R., and Yang, S., SPIE, ISSN 0277-786X, https://doi.org/10.1117/12.2223314, 2016.

Pandey, S. K., Vinoj, V., Landu, K., and Babu, S. S.: Declining pre-monsoon dust loading over South Asia: Signature of a changing regional climate, Scientific Reports, 7, https://doi.org/10.1038/s41598-017-16338-w, 2017.

Pouliot, G., van der Gon, H. A. D., Kuenen, J., Zhang, J., Moran, M. D., and Makar, P. A.: Analysis of the emission inventories and model-ready emission datasets of Europe and North America for phase 2 of the AQMEII project, Atmospheric Environment, 115, 345–360, https://doi.org/10.1016/j.atmosenv.2014.10.061, 2015.

Rafaj, P., Amann, M., Siri, J., and Wuester, H.: Changes in European greenhouse gas and air pollutant emissions 1960–2010: decomposition of determining factors, Climatic Change, 124, 477–504, https://doi.org/10.1007/s10584-013-0826-0, 2013.

Ramachandran, S. and Rupakheti, M.: Trends in physical, optical and chemical columnar aerosol characteristics and radiative effects over South and East Asia: Satellite and ground-based observations, Gondwana Research, 105, 366–387, https://doi.org/10.1016/j.gr.2021.09.016, 2022.

Ramachandran, S., Rupakheti, M., and Lawrence, M. G.: Aerosol-induced atmospheric heating rate decreases over South and East Asia as a result of changing content and composition, Scientific Reports, 10, https://doi.org/10.1038/s41598-020-76936-z, 2020.

Russell, P. B., Bergstrom, R. W., Shinozuka, Y., Clarke, A. D., DeCarlo, P. F., Jimenez, J. L., Livingston, J. M., Redemann, J., Dubovik, O., and Strawa, A.: Absorption Angstrom Exponent in AERONET and related data as an indicator of aerosol composition, Atmospheric Chemistry and Physics, 10, 1155–1169, https://doi.org/10.5194/acp-10-1155-2010, 2010.

Sabetghadam, S., Alizadeh, O., Khoshsima, M., and Pierleoni, A.: Aerosol properties, trends and classification of key types over the Middle East from satellite-derived atmospheric optical data, Atmospheric Environment, 246, 118 100, https://doi.org/10.1016/j.atmosenv.2020.118100, 2021.

Sen, P. K.: Estimates of the Regression Coefficient Based on Kendall's Tau, Journal of the American Statistical Association, 63, 1379–1389, https://doi.org/10.1080/01621459.1968.10480934, 1968.

Shao, Y., Klose, M., and Wyrwoll, K.: Recent global dust trend and connections to climate forcing, Journal of Geophysical Research: Atmospheres, 118, https://doi.org/10.1002/jgrd.50836, 2013.

Sinyuk, A., Holben, B. N., Eck, T. F., Giles, D. M., Slutsker, I., Korkin, S., Schafer, J. S., Smirnov, A., Sorokin, M., and Lyapustin, A.: The AERONET Version 3 aerosol retrieval algorithm, associated uncertainties and comparisons to Version 2, Atmospheric Measurement Techniques, 13, 3375–3411, https://doi.org/10.5194/amt-13-3375-2020, 2020.

Sokhi, R. S., Singh, V., Querol, X., Finardi, S., Targino, A. C., Andrade, M. d. F., Pavlovic, R., Garland, R. M., Massagué, J., Kong, S., Baklanov, A., Ren, L., Tarasova, O., Carmichael, G., Peuch, V.-H., Anand, V., Arbilla, G., Badali, K., Beig, G., Belalcazar, L. C., Bolignano, A., Brimblecombe, P., Camacho, P., Casallas, A., Charland, J.-P., Choi, J., Chourdakis, E., Coll, I., Collins, M., Cyrys, J., da Silva, C. M., Di Giosa, A. D., Di Leo, A., Ferro, C., Gavidia-Calderon, M., Gayen, A., Ginzburg, A., Godefroy, F., Gonzalez, Y. A., Guevara-Luna, M., Haque, S. M., Havenga, H., Herod, D., Hõrrak, U., Hussein, T., Ibarra, S., Jaimes, M., Kaasik, M., Khaiwal, R., Kim, J., Kousa, A., Kukkonen, J., Kulmala, M., Kuula, J., La Violette, N., Lanzani, G., Liu, X., MacDougall, S., Manseau, P. M., Marchegiani, G., McDonald, B., Mishra, S. V., Molina, L. T., Mooibroek, D., Mor, S., Moussiopoulos, N., Murena, F., Niemi, J. V., Noe, S., Nogueira, T., Norman, M., Pérez-Camaño, J. L., Petäjä, T., Piketh, S., Rathod, A., Reid, K., Retama, A., Rivera, O., Rojas, N. Y., Rojas-Quincho, J. P., San José, R., Sánchez, O., Seguel, R. J., Sillanpää, S., Su, Y., Tapper, N., Terrazas, A., Timonen, H., Toscano, D., Tsegas, G., Velders, G. J., Vlachokostas, C., von Schneidemesser, E., VPM, R., Yadav, R., Zalakeviciute, R., and Zavala, M.: A global observational analysis to understand changes in air quality during exceptionally low anthropogenic emission conditions, Environment International, 157, 106 818, https://doi.org/10.1016/j.envint.2021.106818, 2021.

Szymankiewicz, K., Kaminski, J. W., and Struzewska, J.: Application of Satellite Observations and Air Quality Modelling to Validation of NOx Anthropogenic EMEP Emissions Inventory over Central Europe, Atmosphere, 12, 1465, https://doi.org/10.3390/atmos12111465, 2021.

Takamura, T. and Nakajima, T.: Overview of SKYNET and its activities, Optica pura y aplicada, 37, 3303–3308, 2004.

Tao, M., Wang, Z., Tao, J., Chen, L., Wang, J., Hou, C., Wang, L., Xu, X., and Zhu, H.: How Do Aerosol Properties Affect the Temporal Variation of MODIS AOD Bias in Eastern China?, Remote Sensing, 9, 800, https://doi.org/10.3390/rs9080800, 2017.

Tong, D. Q., Lamsal, L., Pan, L., Ding, C., Kim, H., Lee, P., Chai, T., Pickering, K. E., and Stajner, I.: Long-term NOx trends over large cities in the United States during the great recession: Comparison of satellite retrievals, ground observations, and emission inventories, Atmospheric Environment, 107, 70–84, https://doi.org/10.1016/j.atmosenv.2015.01.035, 2015.

Venkataraman, C., Brauer, M., Tibrewal, K., Sadavarte, P., Ma, Q., Cohen, A., Chaliyakunnel, S., Frostad, J., Klimont, Z., Martin, R. V., Millet, D. B., Philip, S., Walker, K., and Wang, S.: Source influence on emission pathways and ambient $PM_{2.5}$ pollution over India (2015–2050), Atmospheric Chemistry and Physics, 18, 8017–8039, https://doi.org/10.5194/acp-18-8017-2018, 2018.

Wang, X., Cai, D., Chen, S., Lou, J., Liu, F., Jiao, L., Cheng, H., Zhang, C., Hua, T., and Che, H.: Spatio-temporal trends of dust emissions triggered by desertification in China, CATENA, 200, 105 160, https://doi.org/10.1016/j.catena.2021.105160, 2021.

Wang, Y., Jiang, J. H., Su, H., Choi, Y.-S., Huang, L., Guo, J., and Yung, Y. L.: Elucidating the Role of Anthropogenic Aerosols in Arctic Sea Ice Variations, Journal of Climate, 31, 99–114, https://doi.org/10.1175/JCLI-D-17-0287.1, 2018.

Wei, J., Li, Z., Lyapustin, A., Sun, L., Peng, Y., Xue, W., Su, T., and Cribb, M.: Reconstructing 1-km-resolution high-quality PM2.5 data records from 2000 to 2018 in China: spatiotemporal variations and policy implications, Remote Sensing of Environment, 252, 112 136, https://doi.org/10.1016/j.rse.2020.112136, 2021a.

Wei, J., Li, Z., Xue, W., Sun, L., Fan, T., Liu, L., Su, T., and Cribb, M.: The ChinaHighPM10 dataset: generation, validation, and spatiotemporal variations from 2015 to 2019 across China, Environment International, 146, 106 290, https://doi.org/10.1016/j.envint.2020.106290, 2021b.

Xia, X.: Variability of aerosol optical depth and Angstrom wavelength exponent derived from AERONET observations in recent decades, Environmental Research Letters, 6, 044 011, https://doi.org/10.1088/1748-9326/6/4/044011, 2011.

Yang, X., Zhao, C., Yang, Y., and Fan, H.: Long-term multi-source data analysis about the characteristics of aerosol optical properties and types over Australia, Atmospheric Chemistry and Physics, 21, 3803–3825, https://doi.org/10.5194/acp-21-3803-2021, 2021.

Yin, S.: Biomass burning spatiotemporal variations over South and Southeast Asia, Environment International, 145, 106 153, https://doi.org/10.1016/j.envint.2020.106153, 2020.

Ying, T., Li, J., Jiang, Z., Liu, G., Zhang, Z., Zhang, L., Dong, Y., and Zhao, C.: Increased aerosol scattering contributes to the recent monsoon rainfall decrease over the Gangetic Plain, Science Bulletin, 68, 2629–2638, https://doi.org/10.1016/j.scib.2023.08.052, 2023.

Yoon, J., von Hoyningen-Huene, W., Kokhanovsky, A. A., Vountas, M., and Burrows, J. P.: Trend analysis of aerosol optical thickness and Ångström exponent derived from the global AERONET spectral observations, Atmospheric Measurement Techniques, 5, 1271–1299, https://doi.org/10.5194/amt-5-1271-2012, 2012.

Yoon, J., Pozzer, A., Chang, D., Lelieveld, J., Kim, J., Kim, M., Lee, Y., Koo, J.-H., Lee, J., and Moon, K.: Trend estimates of AERONET-observed and model-simulated AOTs between 1993 and 2013, Atmospheric Environment, 125, 33–47, https://doi.org/10.1016/j.atmosenv.2015.10.058, 2016.

Yu, X., Nichol, J., Lee, K. H., Li, J., and Wong, M. S.: Analysis of Long-Term Aerosol Optical Properties Combining AERONET Sunphotometer and Satellite-Based Observations in Hong Kong, Remote Sensing, 14, 5220, https://doi.org/10.3390/rs14205220, 2022.

Zhang, L. and Li, J.: Variability of Major Aerosol Types in China Classified Using AERONET Measurements, Remote Sensing, 11, 2334, https://doi.org/10.3390/rs11202334, 2019.

Zhang, Y., Luo, G., and Yu, F.: Seasonal Variations and Long-Term Trend of Dust Particle Number Concentration Over the Northeastern United States, Journal of Geophysical Research: Atmospheres, 124, 13 140–13 155, https://doi.org/10.1029/2019jd031388, 2019.

Zhang, Z., Li, J., Dong, Y., Zhang, C., Ying, T., and Li, Q.: Long-Term Trends in Aerosol Single Scattering Albedo Cause Bias in MODIS Aerosol Optical Depth Trends, IEEE Transactions on Geoscience and Remote Sensing, 62, 1–9, https://doi.org/10.1109/tgrs.2024.3424981, 2024.

Zhao, B., Jiang, J. H., Gu, Y., Diner, D., Worden, J., Liou, K.-N., Su, H., Xing, J., Garay, M., and Huang, L.: Decadal-scale trends in regional aerosol particle properties and their linkage to emission changes, Environmental Research Letters, 12, 054 021, https://doi.org/10.1088/1748-9326/aa6cb2, 2017.

Ångström, A.: On the Atmospheric Transmission of Sun Radiation and on Dust in the Air, Geografiska Annaler, 11, 156, https://doi.org/10.2307/519399, 1929.